

Exact Parameter Identification in PET Pharmacokinetic Modeling Using the Irreversible Two Tissue Compartment Model *

Martin Holler [†] Erion Morina [‡] Georg Schramm [§]

May 29, 2023

Abstract

This work is concerned with the identifiability of metabolic parameters from multi-region measurement data in quantitative PET imaging. It shows that, for the frequently used two-tissue compartment model and under reasonable assumptions, it is possible to uniquely identify metabolic tissue parameters from standard PET measurements, without the need of additional concentration measurements from blood samples. This result, which holds in the idealized, noiseless scenario, indicates that costly concentration measurements from blood samples in quantitative PET imaging can be avoided in principle. The connection to noisy measurement data is made via a consistency result, showing that exact reconstruction is maintained in the vanishing noise limit. Numerical experiments with a regularization approach are further carried out to support these analytic results in an application example.

Keywords: Quantitative PET imaging, two-tissue compartment model, exact reconstruction, Tikhonov regularization, iteratively regularized Gauss Newton method

MSC Codes: 65L09, 94A12, 92C55, 34C60

1 Introduction

Positron emission tomography (PET) is a non-invasive clinical technique that images the four dimensional spatio temporal distribution of a radio tracer in-vivo. In quantitative dynamic PET imaging, after tracer injection, several 3D PET images at different time points are acquired and reconstructed. The injected tracer is supplied to the tissues via the arteries and capillaries. As a response to this “arterial tracer input”, the tracer is exchanged with tissues. This exchange can include reversible and/or irreversible binding and eventually metabolization of the tracer.

Using the right tracer, the time series of reconstructed PET images reflecting the tissue response, a measurement of the arterial tracer input, and a dedicated pharmacokinetic model, it is possible to generate images reflecting certain physiological parameters. Depending on the tracer, these parametric images can reflect e.g. blood flow, blood volume, glucose metabolism or neuro receptor dynamics.

*This work was partly funded by the NIH grants P41-EB017183 and R01-EB031199-02.

[†]Institute of Mathematics and Scientific Computing, University of Graz. MH further is a member of NAWI Graz (www.nawigraz.at) and of BioTechMed Graz (biotechmedgraz.at) (martin.holler@uni-graz.at)

[‡]Institute of Mathematics and Scientific Computing, University of Graz. (erion.morina@uni-graz.at).

[§]Radiological Sciences Laboratory, Stanford University, Stanford, CA, and Department of Imaging and Pathology, KU Leuven, Belgium. (gschra2@stanford.edu)

Pharmacokinetic modeling in PET is commonly performed using compartment models, where the compartments usually reflect tissue subspaces. Example for such subspaces are the extra cellular spaces where the tracer is free or bound.¹ The dynamics between the arterial blood and tissue compartments is typically described using ordinary-differential-equation (ODE) models. For PET tracers with irreversible binding, such as [¹⁸F]Fluorodeoxyglucose (FDG) [14] or [¹¹C]Clorgyline [10], the irreversible two tissue compartment model can be used to describe the tracer dynamics, see Figure 1 for a scheme of this model.

The identification of the kinetic parameters describing the tissue response to the arterial tracer supply in a given region is commonly done using the following input data:

1. The tracer concentration in tissue $C_{\text{tis}}(t)$. This quantity, which is equal to the sum of all the tracer concentrations in all extra-vascular compartments, can be directly obtained from the time series of reconstruction PET images - either on a region-of-interest (ROI) or at voxel level.
2. The arterial “input function” or plasma concentration $C_{\text{art}}(t)$ of the non-metabolized tracer describing the concentration of tracer in the arterial blood plasma that is supplied to tissue and available for exchange (and metabolism). A direct measurement of $C_{\text{art}}(t)$ is complicated. Typically, it is based on an external measurement of a time series of arterial blood samples taken from a patient, e.g. using a well counter. Unfortunately, the total arterial blood tracer concentration $C_{\text{bl}}(t)$ obtained from the well counter measurements usually overestimates $C_{\text{art}}(t)$ since the measured activity of the blood samples also includes activity from radioactive molecules that are not available for exchange with tissue because of (i) parts of the radio tracer being bound to plasma proteins and (ii) activity originating from metabolized tracer molecules that were transferred back from tissue into blood. Measuring the contributions of the latter two effects, summarized in the parent plasma fraction $f(t) = C_{\text{art}}(t)/C_{\text{bl}}(t)$, requires further advanced chemical processing and analysis of the blood samples and is thus time consuming and expensive.

To avoid the necessity of arterial blood sampling, which itself is a very challenging process in clinical routine, many attempts have been made to derive the arterial input function directly from the reconstructed PET images (also called “image-based arterial input function”) by analyzing the tracer concentration in regions of interest of the PET images containing arterial blood, such as the left ventricle, the aorta, or the carotid arteries. Note, however, that by using any image-based approach for the estimation of the arterial input function, the contributions of tracer bound to plasma proteins and metabolized tracers cannot be determined. In other words, any image-based approach can only estimate $C_{\text{bl}}(t)$ instead of $C_{\text{art}}(t)$ since no measurement of the parent plasma fraction $f(t)$ is available.

Motivated by the problem, we consider the question whether the identification of kinetic parameters using data from multiple anatomical regions of interest and the irreversible two tissue compartment model is possible without having access to the common parent plasma fraction $f(t)$ and/or the common total arterial blood tracer concentration $C_{\text{bl}}(t)$.

In existing literature on modeling approaches for quantitative PET, see for instance [17] and [16] for a review, this question has been addressed from a computational perspective. The work [17], for instance, accounts for a low number of measurements of the arterial concentration of non-metabolized PET tracer by using a non-linear mixed effect model for the parent plasma fraction, i.e., the parameters defining the parent plasma fraction are modeled as being partially patient-specific and partially the same for a population sample. Moreover, the general idea of jointly modeling the tissue response in different anatomical regions to obtain unknown common

¹Note that the exact interpretation of the biological meaning of the compartments is highly non-trivial.

parameters or to reduce the variance in the estimated region-dependent parameters has been proposed in [13, 7, 15, 3].

Despite these and many more computational approaches for parameter identification in pharmacokinetic modeling using the irreversible two tissue compartment model, a mathematical analysis about the necessity of measurements of $C_{\text{bl}}(t)$ and/or $f(t)$ for successful parameter identification, even in an idealized, noiseless scenario, does not exist. In addition to that, even in the presence of an arbitrary number of such measurements, it is not clear from an analytical perspective if the tissue parameters in specific ODE-based compartment models can be recovered uniquely.

The aim of this work is to answer these questions. Using a polyexponential parametrization of the arterial plasma concentration, which is frequently used in practice, we prove the following: Let (K_1^i, k_2^i, k_3^i) be the kinetic parameters of different anatomical regions $i = 1, \dots, n$ of the irreversible two tissue compartment model, let T be the number of time-points where PET measurements of the tissue tracer concentration $C_{\text{tis}}(t)$ are available, and let p be the degree of the polyexponential parametrization. Then, if $T \geq 2(p + 3)$, and under some non-restrictive technical conditions as stated in Theorem 14, the parameters k_2^i, k_3^i for $i = 1, \dots, n$ can be identified uniquely already from the available measurements of the tracer concentration in the different tissues without the need for $C_{\text{bl}}(t)$ and $f(t)$. Further, the K_1^i can also be identified already from these measurements up to a constant that is the same for all regions i . In addition, the parameters K_1^i can be identified exactly if a sufficient number of measurements of the total arterial tracer concentration C_{bl} is available, without the need for $f(t)$.

Besides these unique identifiability results that consider the idealized case of a noise-free measurement, we also present analytical results for a standard Tikhonov regularization approach that addresses the situation of noisy measurements. Using classical results from regularization theory, we show that the Tikhonov regularization approach is stable w.r.t. perturbations of the data and, in the vanishing noise limit, allows to approximate the ground-truth tissue parameters. Numerical experiments further illustrate our analytic results also in an application example.

Scope of the paper. In Section 2, we introduce the irreversible two tissue compartment model and provide basic results on explicit solutions both in the general case and in case the arterial concentration is parametrized via polyexponential functions. In Section 3 we present and prove our main results on unique identifiability of parameters. In Section 4 we introduce a Tikhonov regularization approach and show stability and consistency results, and in Sections 5 and 6 we provide a numerical algorithm and numerical experiments for an application example.

2 The irreversible two tissue compartment model

The *irreversible two tissue compartment model* describes the interdependence of the concentration of a radio tracer in the arterial blood plasma and in the extra-vascular compartment, where the latter is further decomposed in a *free* and a *bound* compartment. Note that in the irreversible model, once the radio tracer has reached the bound compartment, it is trapped. A visualization of the model is provided in Figure 1.

We denote by $C_{\text{art}} : [0, \infty) \rightarrow [0, \infty)$ the arterial plasma concentration of the non-metabolized PET tracer. Further, for any anatomical region $i = 1, \dots, n$, we denote by $C_{\text{fr}}^i : [0, \infty) \rightarrow [0, \infty)$ and $C_{\text{bd}}^i : [0, \infty) \rightarrow [0, \infty)$ the free and the bound compartment of the tracer in region i , respectively, and by $C_{\text{tis}}^i = C_{\text{fr}}^i + C_{\text{bd}}^i$ we denote the sum of the two compartments in region i . Using the *irreversible two tissue compartment model*, the interaction of these quantities is

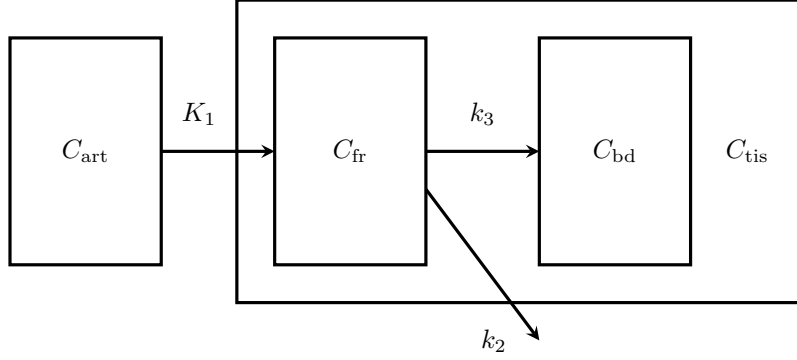


Figure 1: Irreversible two tissue compartment model. The boxes around C_{art} , C_{bd} , C_{fr} and C_{tis} represent the respective concentrations and the arrows between them the directional exchange with the respective rate depicted above or below the corresponding arrow. The box around the C_{bd} and C_{fr} indicates the extra-vascular measurements associated with C_{tis} .

described by the following system of ordinary differential equations (ODEs):

$$\begin{cases} \frac{d}{dt} C_{\text{fr}}^i = K_1^i C_{\text{art}} - (k_2^i + k_3^i) C_{\text{fr}}^i, & t > 0 \\ \frac{d}{dt} C_{\text{bd}}^i = k_3^i C_{\text{fr}}^i, & t > 0 \\ C_{\text{fr}}^i(0) = 0, C_{\text{bd}}^i(0) = 0 \end{cases} \quad (\text{S})$$

Here, the parameters K_1^i , k_2^i and k_3^i are the tracer kinetic parameters that define the interaction of the different compartments in region i .

Our goal is to identify the parameters K_1^i , k_2^i and k_3^i for each $i = 1, \dots, n$. For this, we can use measurements of the $C_{\text{tis}}^i(t_l)$ at different time-points t_1, \dots, t_T obtained from reconstructed PET images at different time points after tracer injection. Further, the parameter identification typically relies on additional measurements related to C_{art} . Here, the standard procedure is to take arterial blood samples and to measure the total activity concentration of the arterial blood samples, given as $C_{\text{bl}} : [0, \infty) \rightarrow [0, \infty)$. The relation of the total concentration C_{bl} to the arterial plasma concentration C_{art} of non-metabolized tracer is described via an unknown parent plasma fraction function $f : [0, \infty) \rightarrow [0, 1]$ with $f(0) = 1$ as

$$C_{\text{art}}(t) = f(t)C_{\text{bl}}(t).$$

As described above, to obtain $f(t)$ and thus $C_{\text{art}}(t)$, a time-consuming and costly plasma separation and metabolite analysis of the blood samples has to be performed.

In order to realize the parameter identification for the ODE model (S) in practice, the involved functionals need to be discretized, e.g., via a suitable parametrization. For the arterial concentration C_{art} , it is standard to use a parametrization via polyexponential functions as defined in the following.

Definition 1 (Polyexponential functions). *We call a function g polyexponential of degree $p \in \mathbb{N}$ if there exist $\lambda_i, \mu_i \in \mathbb{R}$ for $1 \leq i \leq p$ where the $(\mu_i)_{i=1}^p$ are pairwise distinct and $\lambda_i \neq 0$ for all i such that*

$$g(t) = \sum_{i=1}^p \lambda_i e^{\mu_i t}.$$

We write $\deg(g) = p$ and call the zero-function polyexponential of degree zero. By \mathcal{P}_p we denote the set of polyexponential functions of degree less or equal to p , and by $\mathcal{P} = \cup_{p=0}^{\infty} \mathcal{P}_p$ the set of polyexponential functions (of any degree).

Remark 2. It obviously holds that \mathcal{P} is a vector space, and even a subalgebra of $\mathcal{C}^\infty(\mathbb{R})$. It is also worth noting that, as direct consequence of the Stone-Weierstrass Theorem, polyexponential functions are dense in the set of continuous functions on compact domains. Thus, they are a reasonable approximation class also from the analytic perspective.

Modeling C_{art} as polyexponential function already defines a parametrization of the resulting solutions of the ODE system (S). As we will see in Lemma 5 below, the following notion of generalized polyexponential functions is the appropriate notion to describe such solutions.

Definition 3 (Generalized Polyexponential class). *We call a function g generalized polyexponential if it is of the form*

$$g(t) = P_1(t) e^{\mu_1 t} + \dots + P_l(t) e^{\mu_l t},$$

where the $P_1, \dots, P_l \not\equiv 0$ are polynomials of degree $m_1 - 1, \dots, m_l - 1$, respectively, and the μ_j are pairwise distinct constants. We denote the class of such generalized polyexponential functions with polynomials of degree at most $m_1 - 1, \dots, m_l - 1$ by

$$\mathcal{P}[m_1, \dots, m_l].$$

We define the degree of g by

$$\deg(g) = m_1 + \dots + m_l.$$

In case $m_1 = \dots = m_l = 1$ we write $\mathcal{P}_{\deg(g)}$ for the resulting polyexponential class.

The next two results, which follow from standard ODE theory, provide explicitly the solutions $(C_{\text{fr}}, C_{\text{bd}})$ of the ODE system (S), once in the general case and once in case C_{art} is modeled as polyexponential function.

Lemma 4. *Let $C_{\text{art}} : [0, \infty) \rightarrow [0, \infty)$ be continuous, and let the parameters K_1^i , k_2^i and k_3^i be fixed for $i = 1, \dots, n$ such that $k_2^i + k_3^i \neq 0$. Then, for each $i = 1, \dots, n$, the ODE system (S) admits a unique solution $(C_{\text{fr}}^i, C_{\text{bd}}^i)$ that is defined on all of $[0, \infty)$, and such that $C_{\text{tis}}^i = C_{\text{fr}}^i + C_{\text{bd}}^i$ is given as*

$$C_{\text{tis}}^i = \frac{K_1^i k_2^i}{k_2^i + k_3^i} e^{-(k_2^i + k_3^i)t} \int_0^t e^{(k_2^i + k_3^i)s} C_{\text{art}}(s) ds + \frac{K_1^i k_3^i}{k_2^i + k_3^i} \int_0^t C_{\text{art}}(s) ds. \quad (1)$$

Proof. Fix $i \in \{1, \dots, n\}$. From the equation for C_{fr}^i in (S) it immediately follows that

$$C_{\text{fr}}^i(t) = K_1^i e^{-(k_2^i + k_3^i)t} \int_0^t e^{(k_2^i + k_3^i)s} C_{\text{art}}(s) ds. \quad (2)$$

This in turn implies that

$$C_{\text{bd}}^i(t) = -\frac{K_1^i k_3^i}{k_2^i + k_3^i} e^{-(k_2^i + k_3^i)t} \int_0^t e^{(k_2^i + k_3^i)s} C_{\text{art}}(s) ds + \frac{K_1^i k_3^i}{k_2^i + k_3^i} \int_0^t C_{\text{art}}(s) ds$$

and, consequently, that

$$C_{\text{tis}}^i(t) = \frac{K_1^i k_2^i}{k_2^i + k_3^i} e^{-(k_2^i + k_3^i)t} \int_0^t e^{(k_2^i + k_3^i)s} C_{\text{art}}(s) ds + \frac{K_1^i k_3^i}{k_2^i + k_3^i} \int_0^t C_{\text{art}}(s) ds$$

as claimed. \square

Lemma 5. If $C_{art} \in \mathcal{P}_p$ is given as

$$C_{art}(t) = \sum_{j=1}^p \lambda_j e^{\mu_j t},$$

then, for $i \in \{1, \dots, n\}$, C_{tis}^i of Lemma 4 is given as

$$\begin{aligned} C_{tis}^i(t) = & \frac{K_1^i}{k_2^i + k_3^i} \sum_{j=1}^p \left(\frac{k_3^i}{\mu_j} \mathbf{1}_{\{\mu_j \neq 0\}} + \frac{k_2^i}{k_2^i + k_3^i + \mu_j} \mathbf{1}_{\{k_2^i + k_3^i + \mu_j \neq 0\}} \right) \lambda_j e^{\mu_j t} \\ & - \left[\frac{K_1^i k_2^i}{k_2^i + k_3^i} \sum_{\substack{j=1 \\ k_2^i + k_3^i + \mu_j \neq 0}}^p \frac{\lambda_j}{k_2^i + k_3^i + \mu_j} \right] e^{-(k_2^i + k_3^i)t} - \frac{K_1^i k_3^i}{k_2^i + k_3^i} \sum_{\substack{j=1 \\ \mu_j \neq 0}}^p \frac{\lambda_j}{\mu_j} \\ & + \left[\frac{K_1^i k_2^i}{k_2^i + k_3^i} \sum_{\substack{j=1 \\ k_2^i + k_3^i + \mu_j = 0}}^p \lambda_j \right] t e^{-(k_2^i + k_3^i)t} + \frac{K_1^i k_3^i}{k_2^i + k_3^i} \sum_{\substack{j=1 \\ \mu_j = 0}}^p \lambda_j t \quad (3) \end{aligned}$$

Proof. This follows immediately by inserting the representation of C_{art} in (1). \square

Remark 6 (Sign of exponents μ_j). *Note that for the ground truth arterial concentration C_{art} , we will always have $\mu_j < 0$ (in particular $\mu_j \neq 0$) for all $j = 1, \dots, p$, since otherwise this would imply the unphysiological situation that $C_{art}(t) \rightarrow c \neq 0$ for $t \rightarrow \infty$.*

3 Unique identifiability

In view of Lemma 5 from the previous section, it is clear that the question of unique identifiability of the parameters K_1^i , k_2^i and k_3^i from measurements of $C_{tis}^i(t_l)$ at time points t_1, \dots, t_T is related to the question of uniqueness of interpolations with generalized polyexponential functions. A first, existing result in that direction is as follows.

Lemma 7 (Roots of generalized polyexponential functions). *Let P_1, \dots, P_l be polynomials of degree $m_1 - 1, \dots, m_l - 1$ such that at least one of them is not identically zero, and let the constants μ_1, \dots, μ_l be pairwise distinct. Then the function*

$$g(t) = P_1(t) e^{\mu_1 t} + \dots + P_l(t) e^{\mu_l t}$$

admits at most $m_1 + \dots + m_l - 1$ real roots.

Proof. See [12, Exercise 75 (p. 48)]. \square

As a consequence of the previous proposition, we now obtain the following unique interpolation result for generalized polyexponential functions.

Lemma 8 (Unique interpolation). *Let $m_1, \dots, m_p, T \in \mathbb{N}$ be such that*

$$2(m_1 + \dots + m_p) \leq T.$$

Then, for any choice of tuples $(t_i, s_i) \in \mathbb{R}^2$, $i = 1, \dots, T$, with $t_1 < \dots < t_T$, there exists at most one generalized polyexponential function $h \in \mathcal{P}[m_1, \dots, m_p]$ such that

$$h(t_i) = s_i \quad (4)$$

for $l = 1, \dots, T$, i.e., in case

$$h(t) = \sum_{j=1}^p P_j(t) e^{\mu_j t} \quad \text{and} \quad \tilde{h}(t) = \sum_{j=1}^p \tilde{P}_j(t) e^{\tilde{\mu}_j t}$$

are two generalized polyexponential functions with $h, \tilde{h} \in \mathcal{P}[m_1, \dots, m_p]$ fulfilling the interpolation condition (4), then, up to re-indexing,

$$P_j \equiv \tilde{P}_j$$

for all j and $\mu_j = \tilde{\mu}_j$ for all j where $P_j \not\equiv 0$.

Proof. Let both $h, \tilde{h} \in \mathcal{P}[m_1, \dots, m_p]$ fulfill the interpolation condition (4), and, w.l.o.g., assume that $P_j \not\equiv 0$ and $\tilde{P}_j \not\equiv 0$ for all j . Then, $h - \tilde{h} \in \mathcal{P}[m_1, \dots, m_p, m_1, \dots, m_p]$ and $(h - \tilde{h})(t_l) = 0$ for $l = 1, \dots, T$. Lemma 7 then implies that all polynomials appearing in $h - \tilde{h}$ in a representation as in Definition 3 are identically zero. This implies that the $(P_j)_{j=1}^p$ and $(\tilde{P}_j)_{j=1}^p$ coincide up to re-indexing and, likewise, that the corresponding coefficient $(\mu_j)_{j=1}^p$ and $(\tilde{\mu}_j)_{j=1}^p$ where the corresponding polynomials are non-zero coincide as well. \square

Based on this result, we now address the question of uniquely identifying the parameters of the ODE system (S) from time-discrete measurements $C_{\text{tis}}^i(t_1), \dots, C_{\text{tis}}^i(t_T)$ with $i = 1, \dots, n$ and measurements $C_{\text{bl}}(s_1), \dots, C_{\text{bl}}(s_q)$. For this, we first introduce the following notation.

Definition 9 (Parameter configuration). *We call the parameters $p, n \in \mathbb{N}$, $((\lambda_j, \mu_j))_{j=1}^p \in \mathbb{R}^{2 \times p}$, $((K_1^i, k_2^i, k_3^i))_{i=1}^n \in \mathbb{R}^{3 \times n}$ together with the functions $(C_{\text{tis}}^i)_{i=1}^n$ and*

$$C_{\text{art}}(t) = \sum_{j=1}^p \lambda_j e^{\mu_j t}$$

a configuration of the irreversible two tissue compartment model if $\lambda_j \neq 0$ for $j = 1, \dots, p$, the μ_j , $j = 1, \dots, p$ are pairwise distinct, and, for $i = 1, \dots, n$, $C_{\text{tis}}^i = C_{\text{fr}}^i + C_{\text{bd}}^i$ with $(C_{\text{fr}}^i, C_{\text{bd}}^i)$ the solution of the ODE system (S) with arterial concentration C_{art} and parameters K_1^i, k_2^i, k_3^i .

Central for our unique identifiability result will be the following technical assumption on a parameter configuration $(p, n, ((\lambda_j, \mu_j))_{j=1}^p, ((K_1^i, k_2^i, k_3^i))_{i=1}^n, (C_{\text{tis}}^i)_{i=1}^n, C_{\text{art}})$.

$$\left\{ \begin{array}{l} \text{For any } j_0, \text{ there are at least three regions } i_s, s = 1, \dots, 3, \text{ where} \\ k_3^{i_s} \text{ and } k_2^{i_s} + k_3^{i_s} \text{ are each pairwise distinct, } \mu_{j_0} + k_3^{i_s} \neq 0 \\ \text{and either } \mu_{j_0} + k_2^{i_s} + k_3^{i_s} = 0 \text{ or } \sum_{\substack{j=1 \\ \mu_j + k_2^{i_s} + k_3^{i_s} \neq 0}}^p \frac{\lambda_j}{k_2^{i_s} + k_3^{i_s} + \mu_j} \neq 0 \end{array} \right. \quad (\text{A})$$

As the following lemma shows, this assumption holds in case our measurement setup comprises sufficiently many regions where the parameters k_3^i and $k_2^i + k_3^i$ are pairwise distinct. This is reasonable to assume in practice, and also it is a condition which is to be expected: Our unique identifiability result will require a sufficient amount of different regions, and different regions with the same tissue parameter do not provide any additional information on the dynamics of the ODE model.

Lemma 10. *Assume that there are at least $p + 3$ regions i_1, \dots, i_{p+3} , with $p \geq 1$, where each the $k_3^{i_s}$ and the $k_2^{i_s} + k_3^{i_s}$ are pairwise distinct for $s = 1, \dots, p + 3$. Then Assumption (A) holds.*

Proof. For $z \in \mathbb{R}$, note that

$$\left(\prod_{\substack{j=1 \\ \mu_j + z \neq 0}}^p (z + \mu_j) \right) \left(\sum_{\substack{i=1 \\ \mu_i + z \neq 0}}^p \frac{\lambda_i}{z + \mu_i} \right) = \sum_{\substack{i=1 \\ \mu_i + z \neq 0}}^p \lambda_i \prod_{\substack{j=1 \\ j \neq i \\ \mu_j + z \neq 0}}^p (z + \mu_j)$$

is a polynomial in z of degree at most $p-1$. Hence it can admit at most $p-1$ distinct roots. Now since there are at least $p+3$ regions where each the $k_3^{i_s}$ and the $k_2^{i_s} + k_3^{i_s}$ are pairwise distinct, for at least four of them, say i_1, \dots, i_4 , $z = k_2^{i_s} + k_3^{i_s}$ cannot be a root of the above polynomial. Further, for those four regions, since the $k_3^{i_s}$ are pairwise distinct, for any given μ_{j_0} , at most one can be such that $\mu_{j_0} + k_3^{i_s} = 0$. As a consequence, the remaining three are such that the conditions of Assumption (A) hold. \square

Based on Assumption (A), we now obtain the following proposition, which is the technical basis for our subsequent results on unique identifiability.

Proposition 11. *Let $(p, n, ((\lambda_j, \mu_j))_{j=1}^p, ((K_1^i, k_2^i, k_3^i))_{i=1}^n, (C_{tis}^i)_{i=1}^n, C_{art})$ be a configuration of the irreversible two tissue compartment model with $\mu_j \neq 0$ for $j = 1, \dots, p$, $p \geq 3$, $n \geq 3$, $K_1^i, k_2^i, k_3^i > 0$ for all $i = 1, \dots, n$ and such that Assumption (A) holds. Let further t_1, \dots, t_T be distinct points such that*

$$T \geq 2(p+3).$$

Then, with $(\tilde{p}, n, ((\tilde{\lambda}_j, \tilde{\mu}_j))_{j=1}^{\tilde{p}}, ((\tilde{K}_1^i, \tilde{k}_2^i, \tilde{k}_3^i))_{i=1}^n, (\tilde{C}_{tis}^i)_{i=1}^n, \tilde{C}_{art})$ any other configuration of the irreversible two tissue compartment model such that $\tilde{p} \leq p$, $\tilde{k}_3^i \neq 0$ and $\tilde{k}_2^i + \tilde{k}_3^i \neq 0$ for all $i = 1, \dots, n$, it follows from $C_{tis}(t_l) = \tilde{C}_{tis}(t_l)$ for $l = 1, \dots, T$ that

$$\tilde{k}_2^i = k_2^i \text{ and } \tilde{k}_3^i = k_3^i$$

for all $i = 1, \dots, n$, that there exists a constant $\zeta \neq 0$ such that

$$K_1^i = \zeta \tilde{K}_1^i$$

for all $i = 1, \dots, n$, that $p = \tilde{p}$ and that (up to re-indexing)

$$\tilde{\mu}_j = \mu_j \text{ and } \tilde{\lambda}_j = \zeta \lambda_j \text{ for all } j = 1, \dots, p.$$

Proof. Take $(p, n, ((\lambda_j, \mu_j))_{j=1}^p, ((K_1^i, k_2^i, k_3^i))_{i=1}^n, (C_{tis}^i)_{i=1}^n, C_{art})$ and $(\tilde{p}, n, ((\tilde{\lambda}_j, \tilde{\mu}_j))_{j=1}^{\tilde{p}}, ((\tilde{K}_1^i, \tilde{k}_2^i, \tilde{k}_3^i))_{i=1}^n, (\tilde{C}_{tis}^i)_{i=1}^n, \tilde{C}_{art})$ to be two configurations as stated in the proposition, such that in particular

$$C_{tis}^i(t_l) = \tilde{C}_{tis}^i(t_l) \tag{5}$$

for $l = 1, \dots, T$.

Now since $\mu_j \neq 0$ for all $j = 1, \dots, p$, we obtain the following representation of C_{tis}^i :

$$C_{\text{tis}}^i(t) = \frac{K_1^i}{k_2^i + k_3^i} \sum_{j=1}^p \left(\frac{k_3^i}{\mu_j} + \frac{k_2^i}{k_2^i + k_3^i + \mu_j} \mathbf{1}_{\{k_2^i + k_3^i + \mu_j \neq 0\}} \right) \lambda_j e^{\mu_j t} \\ - \left[\frac{K_1^i k_2^i}{k_2^i + k_3^i} \sum_{\substack{j=1 \\ k_2^i + k_3^i + \mu_j \neq 0}}^p \frac{\lambda_j}{k_2^i + k_3^i + \mu_j} \right] e^{-(k_2^i + k_3^i)t} - \frac{K_1^i k_3^i}{k_2^i + k_3^i} \sum_{j=1}^p \frac{\lambda_j}{\mu_j} \\ + \left[\frac{K_1^i k_2^i}{k_2^i + k_3^i} \sum_{\substack{j=1 \\ k_2^i + k_3^i + \mu_j = 0}}^p \lambda_j \right] t e^{-(k_2^i + k_3^i)t}. \quad (6)$$

In particular, for any region $i \in \{1, \dots, n\}$, the coefficients of $e^{\mu_j t}$ for $j = 1, \dots, p$ in this representation are given as either

$$\frac{K_1^i \lambda_j k_3^i}{\mu_j (k_2^i + k_3^i)} \neq 0$$

in case $k_2^i + k_3^i + \mu_j = 0$ or

$$\frac{K_1^i \lambda_j (\mu_j + k_3^i)}{\mu_j (k_2^i + k_3^i + \mu_j)}$$

otherwise. The latter can only be zero if $\mu_j + k_3^i = 0$, which can happen for at most one \hat{j} by the $(\mu_j)_j$ being pairwise distinct. Since $p \geq 3$ by assumption, this implies in particular that C_{tis}^i is a non-zero function for any i . As a consequence of (5), the condition $T \geq 2(p+3)$ and the unique interpolation result of Lemma 8, this implies that \tilde{C}_{tis}^i is a non-zero function, such that in particular $\tilde{K}_1^i \neq 0$ for all $i \in \{1, \dots, n\}$. Together with the assumption that $\tilde{k}_3^i \neq 0$ for all i , we also obtain that $\tilde{\mu}_j \neq 0$ for all j , since otherwise \tilde{C}_{tis}^i would have a non-zero coefficient of t . As a consequence, also \tilde{C}_{tis}^i admits a representation as in (6).

Uniqueness of the exponents $(\mu_j)_{j=1}^p$. As first step, we now aim to show that $\tilde{p} = p$ (in particular $\tilde{\lambda}_j \neq 0$ for all j) and that (up to re-indexing) $\mu_j = \tilde{\mu}_j$ for all $j = 1, \dots, p$.

We start with a region $i_0 \in \{1, \dots, n\}$. In this region, as argued above, the coefficients of the $e^{\mu_j t}$ for $j = 1, \dots, p$ can be zero for at most one \hat{j} . Since further at most one j_0 can be such that $\mu_{j_0} = -(\tilde{k}_2^{i_0} + \tilde{k}_3^{i_0})$, the unique interpolation result of Lemma 8 applied to $C_{\text{tis}}^{i_0}$ and $\tilde{C}_{\text{tis}}^{i_0}$ yields that $\tilde{p} \geq p - 2 \geq 1$ and that (up to re-indexing) $\mu_j = \tilde{\mu}_j$ for all $j \notin \{\hat{j}, j_0\}$.

Now as a consequence of Assumption A, we can pick a region $i_1 \neq i_0$ with $k_3^{i_1} \neq k_3^{i_0}$ where $\mu_{j_0} + k_3^{i_1} \neq 0$. Since already $\mu_{\hat{j}} + k_3^{i_0} = 0$ it further must hold that $\mu_{\hat{j}} + k_3^{i_1} \neq 0$. This means that the coefficients of both $e^{\mu_{\hat{j}} t}$ and $e^{\mu_{j_0} t}$ in the representation of $C_{\text{tis}}^{i_1}$ as in (3) are non-zero. Again by the μ_j being pairwise distinct, this implies that $\tilde{p} \geq p - 1$ and that (up to re-indexing) either $\mu_{\hat{j}} = \tilde{\mu}_{\hat{j}}$ or $\mu_{j_0} = \tilde{\mu}_{j_0}$.

Case I. Assume that $\mu_{\hat{j}} = \tilde{\mu}_{\hat{j}}$. If also $\mu_{j_0} = \tilde{\mu}_{j_0}$ (and $\tilde{p} \geq p$) we are done with this step, so assume the contrary.

Now as a consequence of Assumption A, we can pick i_2, i_3 and i_4 to be regions where $\mu_{j_0} + k_3^{i_l} \neq 0$ and either $\mu_{j_0} + k_2^{i_l} + k_3^{i_l} = 0$ or the coefficient of $e^{-(k_2^{i_l} + k_3^{i_l})t}$ in the representation of $C_{\text{tis}}^{i_l}$ is non-zero. The fact that $\mu_{j_0} + k_3^{i_l} \neq 0$, together with $\mu_{j_0} \neq \tilde{\mu}_{j_0}$ by assumption, further yields that $\mu_{j_0} = -(\tilde{k}_2^{i_l} + \tilde{k}_3^{i_l})$ for all $l = 2, 3, 4$.

Now we argue that in each region i_l with $l = 2, 3, 4$, it must hold that either $-(k_2^{i_l} + k_3^{i_l}) = \tilde{\mu}_{j_0}$ or $k_2^{i_l} + k_3^{i_l} = \tilde{k}_2^{i_l} + \tilde{k}_3^{i_l}$. To this aim, we make another case distinction for a fixed $l \in \{2, 3, 4\}$.

Case I.A Assume that there exists j_l with $k_2^{i_l} + k_3^{i_l} + \mu_{j_l} = 0$. From the fact that this can happen at most for one j_l and that $\lambda_{j_l} \neq 0$, it follows that the coefficient of $te^{-(k_2^{i_l} + k_3^{i_l})t}$ is non-zero. Consequently, it follows from the unique interpolation result that $k_2^{i_l} + k_3^{i_l} = \tilde{k}_2^{i_l} + \tilde{k}_3^{i_l}$ as claimed.

Case I.B Assume that $k_2^{i_l} + k_3^{i_l} + \mu_j \neq 0$ for all j . This means that $\tilde{\mu}_j = \mu_j \neq -(k_2^{i_l} + k_3^{i_l})$ for all $j \neq j_0$. But since the coefficient of $e^{-(k_2^{i_l} + k_3^{i_l})t}$ is non-zero, by the unique interpolation result it must hence hold that either $-(k_2^{i_l} + k_3^{i_l}) = \tilde{\mu}_{j_0}$ or $k_2^{i_l} + k_3^{i_l} = \tilde{k}_2^{i_l} + \tilde{k}_3^{i_l}$ as claimed. This concludes Case I.B.

Now given that either $-(k_2^{i_l} + k_3^{i_l}) = \tilde{\mu}_{j_0}$ or $k_2^{i_l} + k_3^{i_l} = \tilde{k}_2^{i_l} + \tilde{k}_3^{i_l}$ for all $l = 2, 3, 4$, one of the two cases must happen at least twice. By uniqueness of the $k_2^{i_l} + k_3^{i_l}$ for $l = 2, 3, 4$, only $k_2^{i_l} + k_3^{i_l} = \tilde{k}_2^{i_l} + \tilde{k}_3^{i_l}$ can happen twice. On the other hand, since $\mu_{j_0} = -(\tilde{k}_2^{i_l} + \tilde{k}_3^{i_l})$ for all $l = 2, 3, 4$, this yields that at least two $k_2^{i_l} + k_3^{i_l}$ coincide, which is a contradiction. Hence Case I is complete.

Case II. Assume that $\mu_{j_0} = \tilde{\mu}_{j_0}$. In this case, interchanging the role of μ_{j_0} and $\mu_{\hat{j}}$, we can argue that $\mu_{\hat{j}} = \tilde{\mu}_{\hat{j}}$ exactly as in Case I.

Uniqueness of at least three of the exponents $k_2^i + k_3^i$. Let i_0 be any region such that either $\mu_{j_0} + k_2^{i_0} + k_3^{i_0} = 0$ for some $j_0 \in \{1, \dots, p\}$ (such that the coefficient of $te^{-(k_2^{i_0} + k_3^{i_0})t}$ in the representation of $C_{\text{tis}}^{i_0}$ is non-zero) or the coefficient of $e^{-(k_2^{i_0} + k_3^{i_0})t}$ in the representation of $C_{\text{tis}}^{i_0}$ is non-zero, and note that, according to Assumption A, at least three such regions exist.

Case I. Assume that there exists $j_0 \in \{1, \dots, p\}$ such that $k_2^{i_0} + k_3^{i_0} + \mu_{j_0} = 0$. This implies that the coefficient of $te^{-(k_2^{i_0} + k_3^{i_0})t}$ is non-zero and, consequently, already that $k_2^{i_0} + k_3^{i_0} = \tilde{k}_2^{i_0} + \tilde{k}_3^{i_0}$ by uniqueness of exponents.

Case II. Assume that $k_2^{i_0} + k_3^{i_0} + \mu_j \neq 0$ for all $j = 1, \dots, p$. Now since then the coefficient of $e^{-(k_2^{i_0} + k_3^{i_0})t}$ is non-zero by assumption, $-(k_2^{i_0} + k_3^{i_0})$ must match some exponent in the representation of $\tilde{C}_{\text{tis}}^{i_0}$. It cannot match any of the $\tilde{\mu}_j = \mu_j$ since $k_2^{i_0} + k_3^{i_0} + \mu_j \neq 0$ for all $j = 1, \dots, p$, hence again $k_2^{i_0} + k_3^{i_0} = \tilde{k}_2^{i_0} + \tilde{k}_3^{i_0}$ follows.

Uniqueness of at least three of the exponents k_2^i, k_3^i . First note that for any $i \in \{1, \dots, n\}$ where $\tilde{k}_2^i + \tilde{k}_3^i = k_2^i + k_3^i$, from the unique interpolation result, it follows that

$$K_1^i \lambda_j (\mu_j + k_3^i) = \tilde{K}_1^i \tilde{\lambda}_j (\mu_j + \tilde{k}_3^i) \quad (7)$$

for all $j = 1, \dots, p$. Indeed, in case $k_2^i + k_3^i + \mu_j = 0$, it follows from the coefficients of $te^{-(k_2^i + k_3^i)t}$ in C_{tis}^i and \tilde{C}_{tis}^i being equal that

$$\frac{K_1^i k_2^i \lambda_j}{k_2^i + k_3^i} = \frac{\tilde{K}_1^i \tilde{k}_2^i \tilde{\lambda}_j}{\tilde{k}_2^i + \tilde{k}_3^i},$$

which implies that $K_2^i k_2^i \lambda_j = \tilde{K}_2^i \tilde{k}_2^i \tilde{\lambda}_j$ and, using that $k_2^i = -\mu_j - k_3^i$ and $\tilde{k}_2^i = -\mu_j - \tilde{k}_3^i$, further yields $K_1^i \lambda_j (\mu_j + k_3^i) = \tilde{K}_1^i \tilde{\lambda}_j (\mu_j + \tilde{k}_3^i)$ as claimed.

In the other case, the equality (7) follows directly from the coefficients of $e^{\mu_j t}$ in C_{tis}^i and \tilde{C}_{tis}^i being equal.

Now let i_0 be any region where $\tilde{k}_2^{i_0} + \tilde{k}_3^{i_0} = k_2^{i_0} + k_3^{i_0}$, and for which we want to show that $k_2^{i_0} = \tilde{k}_2^{i_0}$ and $k_3^{i_0} = \tilde{k}_3^{i_0}$. Again we consider several cases.

Case I. Assume that there exists $j_0 \in \{1, \dots, p\}$ such that $\mu_{j_0} + k_3^{i_0} = 0$. In this case, it follows from (7) that also $\mu_{j_0} + \tilde{k}_3^{i_0} = 0$ (note that $\tilde{\lambda}_{j_0} \neq 0$ and $\tilde{K}_1^{i_0} \neq 0$ since $\tilde{p} = p$), hence $k_3^{i_0} = \tilde{k}_3^{i_0}$ and, consequently, $k_2^{i_0} = \tilde{k}_2^{i_0}$ holds.

Case II. Assume that $\mu_j + k_3^{i_0} \neq 0$ for all j . In this case, using Assumption A and the previous step, we can select i_1 to be a second region where again $\tilde{k}_2^{i_1} + \tilde{k}_3^{i_1} = k_2^{i_1} + k_3^{i_1}$ and such that the $k_3^{i_0} \neq k_3^{i_1}$. We have two cases.

Case II.A Assume that there exists $j_1 \in \{1, \dots, p\}$ such that $\mu_{j_1} + k_3^{i_1} = 0$. As in Case I above, this implies that $k_3^{i_1} = \tilde{k}_3^{i_1}$. Further, choosing two indices $j_2, j_3 \in \{1, \dots, p\}$ such that j_1, j_2, j_3 are pairwise distinct, it follows that $\mu_{j_2} + k_3^{i_1} \neq 0$ and $\mu_{j_3} + k_3^{i_1} \neq 0$ by the μ_j being different. Using (7) and $k_3^{i_1} = \tilde{k}_3^{i_1}$ this implies

$$K_1^{i_1} \lambda_{j_1} = \tilde{K}_1^{i_1} \tilde{\lambda}_{j_1} \quad K_1^{i_1} \lambda_{j_2} = \tilde{K}_1^{i_1} \tilde{\lambda}_{j_2}$$

Using that the $\tilde{K}_1^{i_1}, \tilde{K}_1^{i_2}$ cannot be zero, these two equations imply

$$\frac{\tilde{\lambda}_{j_1}}{\lambda_{j_1}} = \frac{\tilde{\lambda}_{j_2}}{\lambda_{j_2}}.$$

Combining this with the equations (7) for $i = i_0$ and $j = j_2, j_3$ we obtain

$$\frac{\mu_{j_3} + \tilde{k}_3^{i_0}}{\mu_{j_3} + k_3^{i_0}} = \frac{\mu_{j_2} + \tilde{k}_3^{i_0}}{\mu_{j_2} + k_3^{i_0}}$$

Reformulating this equation and using that $\mu_{j_2} \neq \mu_{j_3}$ this implies that $k_3^{i_0} = \tilde{k}_3^{i_0}$ and, consequently, $k_3^{i_0} = \tilde{k}_3^{i_0}$ holds.

Case II.B Assume that $\mu_j + k_3^{i_1} \neq 0$ for all j . Defining $\Lambda_j = \tilde{\lambda}_j / \lambda_j$, we then obtain from (7) for pairwise distinct $j_1, j_2, j_3 \in \{1, \dots, p\}$ that

$$\Lambda_{j_1} \frac{\mu_{j_1} + \tilde{k}_3^{i_s}}{\mu_{j_1} + k_3^{i_s}} = \Lambda_{j_2} \frac{\mu_{j_2} + \tilde{k}_3^{i_s}}{\mu_{j_2} + k_3^{i_s}} = \Lambda_{j_3} \frac{\mu_{j_3} + \tilde{k}_3^{i_s}}{\mu_{j_3} + k_3^{i_s}}.$$

for $s = 0, 1$. From this, we conclude that

$$0 = \frac{\mu_{j_r} + \tilde{k}_3^{i_0}}{\mu_{j_r} + k_3^{i_0}} \frac{\mu_{j_s} + \tilde{k}_3^{i_1}}{\mu_{j_s} + k_3^{i_1}} - \frac{\mu_{j_r} + \tilde{k}_3^{i_1}}{\mu_{j_r} + k_3^{i_1}} \frac{\mu_{j_s} + \tilde{k}_3^{i_0}}{\mu_{j_s} + k_3^{i_0}} \quad (8)$$

for $r, s \in \{1, 2, 3\}$ with $r \neq s$.

Multiplying (8) with the denominator $(\mu_{j_r} + k_3^{i_0})(\mu_{j_s} + k_3^{i_1})(\mu_{j_r} + k_3^{i_1})(\mu_{j_s} + k_3^{i_0})$ and further dividing by $(\mu_{j_r} - \mu_{j_s})$ we obtain

$$0 = \mu_{j_r} \mu_{j_s} \left(\tilde{k}_3^{i_0} - \tilde{k}_3^{i_1} + k_3^{i_1} - k_3^{i_0} \right) + (\mu_{j_r} + \mu_{j_s}) \left(k_3^{i_1} \tilde{k}_3^{i_0} - k_3^{i_0} \tilde{k}_3^{i_1} \right) \\ + (k_3^{i_1} - k_3^{i_0}) \tilde{k}_3^{i_0} \tilde{k}_3^{i_1} + \left(\tilde{k}_3^{i_0} - \tilde{k}_3^{i_1} \right) k_3^{i_0} k_3^{i_1}$$

for $r, s \in \{1, 2, 3\}$ with $r \neq s$. Subtracting the above equation for $(r, s) = (1, 3)$ from the same equation for $(r, s) = (1, 2)$ and dividing by $(\mu_{j_2} - \mu_{j_3})$ we obtain

$$0 = \mu_{j_1} \left(\tilde{k}_3^{i_0} - \tilde{k}_3^{i_1} + k_3^{i_1} - k_3^{i_0} \right) + \left(k_3^{i_1} \tilde{k}_3^{i_0} - k_3^{i_0} \tilde{k}_3^{i_1} \right). \quad (9)$$

Similarly, subtracting the above equation for $(r, s) = (2, 3)$ from the same equation for $(r, s) = (2, 1)$ and dividing by $(\mu_{j_1} - \mu_{j_3})$ we obtain

$$0 = \mu_{j_2} \left(\tilde{k}_3^{i_0} - \tilde{k}_3^{i_1} + k_3^{i_1} - k_3^{i_0} \right) + \left(k_3^{i_1} \tilde{k}_3^{i_0} - k_3^{i_0} \tilde{k}_3^{i_1} \right). \quad (10)$$

Combining the last two equations and using that $\mu_{j_1} \neq \mu_{j_2}$ we obtain

$$\tilde{k}_3^{i_0} - k_3^{i_0} = \tilde{k}_3^{i_1} - k_3^{i_1},$$

i.e., $\tilde{k}_3^{i_0} = k_3^{i_0} + \epsilon$ and $\tilde{k}_3^{i_1} = k_3^{i_1} + \epsilon$ for $\epsilon \in \mathbb{R}$. Inserting this into (9) we obtain

$$\epsilon(k_3^{i_1} - k_3^{i_0}) = 0$$

which, together with $k_3^{i_1} \neq k_3^{i_0}$, yields $\epsilon = 0$ and hence in particular $k_3^{i_0} = \tilde{k}_3^{i_0}$ as desired. Together with $k_2^{i_0} + k_3^{i_0} = \tilde{k}_2^{i_0} + \tilde{k}_3^{i_0}$ this yields that also $k_2^{i_0} = \tilde{k}_2^{i_0}$.

Uniqueness of the remaining k_2^i, k_3^i and of the K_1^i up to a constant factor. Take i_0 to be a region where $\tilde{k}_2^{i_0} = k_2^{i_0}$ (we know already that such a region exists). It then follows from (7) that

$$K_1^{i_0} \lambda_j = \tilde{K}_1^{i_0} \tilde{\lambda}_j. \quad (11)$$

for $j = 1, \dots, p$. Thus, with $\zeta := K_1^{i_0} / \tilde{K}_1^{i_0} \neq 0$, we have that $\tilde{\lambda}_j = \zeta \lambda_j$ for all j . We now aim to show that, for all $i \in \{1, \dots, n\}$, $k_2^i = \tilde{k}_2^i$, $k_3^i = \tilde{k}_3^i$ and $K_1^i = \zeta \tilde{K}_1^i$.

Consider $i \in \{1, \dots, n\}$ fixed. To simplify notation, we drop here the index i , e.g., we write $K_1 = K_1^i$, $k_2 = k_2^i$ and $k_3 = k_3^i$ and similar for $\tilde{K}_1, \tilde{k}_2, \tilde{k}_3$.

In case $k_2 + k_3 + \mu_{j_0} = 0$ for some j_0 , we know already from the previous step that $k_2 = \tilde{k}_2$ and $k_3 = \tilde{k}_3$, such that, from equating coefficients in the representations of C_{tis} and \tilde{C}_{tis} , we get

$$K_1 \lambda_j = \tilde{K}_1 \tilde{\lambda}_j = \tilde{K}_1 \zeta \lambda_j,$$

such that also $K_1 = \zeta \tilde{K}_1$ as desired.

In the other case that $k_2 + k_3 + \mu_j \neq 0$ for all j , we get from equating coefficients in the representations of C_{tis} and \tilde{C}_{tis} , using $\tilde{\lambda}_j = \zeta \lambda_j$, that

$$\frac{\tilde{K}_1 \zeta (\mu_j + \tilde{k}_3)}{\tilde{k}_2 + \tilde{k}_3 + \mu_j} = \frac{K_1 (\mu_j + k_3)}{k_2 + k_3 + \mu_j} := z_j \quad (12)$$

for $j = 1, \dots, p$, where the z_j are pairwise distinct by the μ_j being pairwise distinct. Now we show that, from (12), it follows that $\zeta \tilde{K}_1 = K_1$, $\tilde{k}_2 = k_2$ and $\tilde{k}_3 = k_3$. For this, we again need to distinguish several cases.

Case I. $\tilde{k}_3 + \mu_{j_0} = 0$ for at least one $j_0 \in \{1, 2, 3\}$. This implies that also $k_3 + \mu_{j_0} = 0$ and hence that $\tilde{k}_3 = k_3$. Considering $j_1, j_2 \in \{1, 2, 3\} \setminus \{j_0\}$ with $j_1 \neq j_2$ it follows from the μ_j being pairwise distinct that $k_3 + \mu_{j_s} \neq 0$ for $s = 1, 2$, which implies that also $\tilde{k}_3 + \mu_{j_s} \neq 0$ for $s = 1, 2$ and, consequently, that

$$\zeta \tilde{K}_1 = \frac{z_{j_s}}{\mu_{j_s} + k_3} \tilde{k}_2 + \frac{z_{j_s}}{\mu_{j_s} + k_3} (\mu_{j_s} + k_3) \quad (13)$$

for $s = 1, 2$. Now if $\frac{z_{j_1}}{\mu_{j_1} + k_3} \neq \frac{z_{j_2}}{\mu_{j_2} + k_3}$, one may derive $\tilde{k}_2 = k_2$ by rearranging the terms in (13) for $s = 1, 2$. Hence, by inserting the obtained equalities $\tilde{k}_2 = k_2$ and $\tilde{k}_3 = k_3$ in (12) we further deduce $\zeta \tilde{K}_1 = K_1$. If, on the other hand $\frac{z_{j_1}}{\mu_{j_1} + k_3} = \frac{z_{j_2}}{\mu_{j_2} + k_3}$ we can plug in the definition of z_{j_1}, z_{j_2} and obtain

$$\frac{K_1}{k_2 + k_3 + \mu_{j_1}} = \frac{K_1}{k_2 + k_3 + \mu_{j_2}},$$

which yields $\mu_{j_1} = \mu_{j_2}$ and hence a contradiction.

Case II. $\tilde{k}_3 + \mu_j \neq 0$ for all $j = 1, 2, 3$. In this case we can reformulate (12) to obtain

$$\zeta \tilde{K}_1 = z_j \frac{\tilde{k}_2 + \tilde{k}_3 + \mu_j}{\mu_j + \tilde{k}_3} \quad (14)$$

for all $j = 1, 2, 3$. In particular, this yields

$$z_1 \frac{\tilde{k}_2 + \tilde{k}_3 + \mu_1}{\mu_1 + \tilde{k}_3} = z_2 \frac{\tilde{k}_2 + \tilde{k}_3 + \mu_2}{\mu_2 + \tilde{k}_3}.$$

Now if $z_1(\mu_2 + \tilde{k}_3) = z_2(\mu_1 + \tilde{k}_3)$, this implies $\mu_1 = \mu_2$ and hence a contradiction. Thus, using that $z_1(\mu_2 + \tilde{k}_3) \neq z_2(\mu_1 + \tilde{k}_3)$ we can reformulate the previous equation to obtain

$$\tilde{k}_2 = \frac{(z_2 - z_1)(\mu_2 + \tilde{k}_3)(\mu_1 + \tilde{k}_3)}{z_1(\mu_2 + \tilde{k}_3) - z_2(\mu_1 + \tilde{k}_3)}. \quad (15)$$

Now, in equation (12) for $j = 3$, replacing $\zeta \tilde{K}_1$ by the equality (14) for $j = 2$ and plugging in the expression (15) for \tilde{k}_2 we obtain, after some reformulations,

$$\begin{aligned} \tilde{k}_3[(z_3 - z_2)(\mu_2 - \mu_1)z_1 - (z_2 - z_1)(\mu_3 - \mu_2)z_3] = \\ = (z_2 - z_1)\mu_1[z_2\mu_3 - z_3\mu_2] - (z_3 - z_2)\mu_3[z_1\mu_2 - z_2\mu_1]. \end{aligned} \quad (16)$$

Using the definition of the \tilde{z}_j in (12) we derive that the factor after \tilde{k}_3 in (16) corresponds to the term

$$K_1^2 k_2 \frac{(\mu_2 - \mu_1)(\mu_3 - \mu_2)(\mu_1 - \mu_3)}{(k_2 + k_3 + \mu_1)(k_2 + k_3 + \mu_2)(k_2 + k_3 + \mu_3)} \neq 0$$

which is nonzero by the μ_j being pairwise distinct. Thus, again plugging in the definition of the \tilde{z}_j in (12) and rearranging the terms in (16) yields $\tilde{k}_3 = k_3$ after some computations and, consequently, also $\tilde{k}_2 = k_2$ and $\zeta \tilde{K}_1 = K_1$ by the previous considerations.

As a consequence, the remaining $\zeta \tilde{K}_1^i, \tilde{k}_2^i, \tilde{k}_3^i$ considered in this final part of the proof are uniquely determined as $\zeta \tilde{K}_1^i = K_1^i, \tilde{k}_2^i = k_2^i$ and $\tilde{k}_3^i = k_3^i$ \square

The previous result shows that, already under knowledge of $C_{\text{tis}}^i(t_i)$ for $i = 1, \dots, n$ and sufficiently many distinct time-points t_i , the coefficients k_2^i, k_3^i and the coefficients K_1^i can be determined uniquely and uniquely up to a constant, respectively. Considering the ODE system (S), it is clear that this result cannot be improved in the sense that the constant factor of K_1^i cannot be determined without any knowledge of C_{art} (since one can always divide all K_1^i by a constant and multiply C_{art} by the same constant).

In case one aims to determine all parameters of a given configuration uniquely, some additional measurements related to C_{art} are necessary. It is easy to see that a single, non-zero measurement of C_{art} , for instance, would suffice. Indeed, given the value of a ground truth $\hat{C}_{\text{art}}(\hat{s}) \neq 0$ at some time-point \hat{s} , the equality $C_{\text{art}}(\hat{s}) = \hat{C}_{\text{art}}(\hat{s}) = \tilde{C}_{\text{art}}(\hat{s})$ together with the result from Proposition 11 immediately imply that $\zeta = 1$ such that all parameters are uniquely defined.

In current practice, indeed measurements of C_{art} are obtained via an expensive blood-sample analysis, and used for parameter identification, see for instance [17]. As discussed in the introduction, however, in contrast to obtaining measurements of C_{art} , it is much simpler to obtain measurements of the total concentration C_{bl} , where $C_{\text{art}} = f C_{\text{bl}}$ with the unknown parent plasma fraction f .

As the following result shows, measurements of C_{bl} only are indeed sufficient to uniquely identify all remaining parameters, provided that one has sufficiently many measurements in relation to a parametrization of f . To formulate this, we need a notion of parametrization of the parent plasma fractions.

Definition 12 (Parametrized function class for parent plasma fractions). *For any $q \in \mathbb{N}$, we say that a set of functions $F_q \subset \{f : \mathbb{R} \rightarrow \mathbb{R}\}$ is a degree- q parametrized set if for any $f, \tilde{f} \in F_q$ and $\lambda \in \mathbb{R}$ it holds that $\lambda f - \tilde{f}$ attaining zero at q distinct points implies that $\lambda = 1$ and $f = \tilde{f}$.*

Simple examples of degree- q parametrized sets of functions are polynomials of degree $q - 1$ that satisfy $f(x_0) = c$ for some given $x_0, c \in \mathbb{R}$ with $c \neq 0$ or polyexponential functions of degree $q/2$ (if q is even) that satisfy $f(x_0) = c$ for some given $x_0, c \in \mathbb{R}$ with $c \neq 0$. The latter is a frequently used type of parametrization for parent plasma functions (where $f(0) = 1$ is required), see for instance [17].

Proposition 13. *In the situation of Proposition 11, assume in addition that $f, \tilde{f} : \mathbb{R} \rightarrow \mathbb{R}$ are parent plasma fractions contained in the same degree- q parametrized set of functions, and are such that*

$$C_{\text{art}}(s_l) = f(s_l)C_{\text{bl}}(s_l) \text{ and } \tilde{C}_{\text{art}}(s_l) = \tilde{f}(s_l)C_{\text{bl}}(s_l) \text{ for } l = 1, \dots, q,$$

with s_1, s_2, \dots, s_q being q different points, and $C_{\text{bl}}(s_l) \neq 0$ given for $l = 1, \dots, q$. Then, all assertions of Proposition 11 hold with $\zeta = 1$, and further

$$f = \tilde{f}.$$

Proof. Proposition 11 already implies that $\tilde{C}_{\text{art}} = \zeta C_{\text{art}}$. Using that, by assumption,

$$\zeta f(s_l)C_{\text{bl}}(s_l) = \zeta C_{\text{art}}(s_l) = \tilde{C}_{\text{art}}(s_l) = \tilde{f}(s_l)C_{\text{bl}}(s_l),$$

we obtain $(\zeta f - \tilde{f})(s_l) = 0$ for $l = 1, \dots, q$. Since $f, \tilde{f} : \mathbb{R} \rightarrow \mathbb{R}$ are parent plasma fractions contained in the same degree- q parametrized set, this implies that $\zeta = 1$ and $f = \tilde{f}$ as claimed. \square

The following theorem now summarizes results of the previous two propositions in view of practical applications.

Theorem 14. *Let $(p, n, ((\lambda_j, \mu_j))_{j=1}^p, ((K_1^i, k_2^i, k_3^i))_{i=1}^n, (C_{\text{tis}}^i)_{i=1}^n, C_{\text{art}})$ be a ground-truth configuration of the irreversible two tissue compartment model such that*

1. $p \geq 3$, $n \geq 3$ and $K_1^i, k_2^i, k_3^i > 0$ for all $i = 1, \dots, n$,
2. *There are at least $p + 3$ regions i_1, \dots, i_{p+3} where each the $k_3^{i_s}$ and the $k_2^{i_s} + k_3^{i_s}$ are pairwise distinct for $s = 1, \dots, p + 3$.*

Let further be $C_{\text{bl}} : [0, \infty) \rightarrow [0, \infty)$ be the ground truth total concentration.

Then, for any other parameter configuration $(\tilde{p}, n, ((\tilde{\lambda}_j, \tilde{\mu}_j))_{j=1}^{\tilde{p}}, ((\tilde{K}_1^i, \tilde{k}_2^i, \tilde{k}_3^i))_{i=1}^n, (\tilde{C}_{\text{tis}}^i)_{i=1}^n, \tilde{C}_{\text{art}})$ such that the conditions 1) and 2) above also hold, it follows from

$$C_{\text{tis}}(t_l) = \tilde{C}_{\text{tis}}(t_l) \text{ for } l = 1, \dots, T$$

with $T \geq \max\{2(p + 3), 2(\tilde{p} + 3)\}$ and the t_1, \dots, t_T pairwise distinct, that, for some constant $\zeta \neq 0$,

$$K_1^i = \zeta \tilde{K}_1^i, k_2^i = \tilde{k}_2^i \text{ and } k_3^i = \tilde{k}_3^i \text{ for all } i = 1, \dots, n,$$

that $p = \tilde{p}$, and that (up to re-indexing)

$$\tilde{\mu}_j = \mu_j \text{ and } \tilde{\lambda}_j = \zeta \lambda_j \text{ for all } j = 1, \dots, p.$$

If further $f : [0, \infty) \rightarrow [0, \infty)$ is a ground-truth parent plasma fraction in a degree- q parametrized set of functions and $\tilde{f} : [0, \infty) \rightarrow [0, \infty)$ is a parent plasma fraction in the same degree- q parametrized set of functions such that

$$C_{art}(s_l) = f(s_l)C_{bl}(s_l) \text{ and } \tilde{C}_{art}(s_l) = \tilde{f}(s_l)C_{bl}(s_l) \text{ for } l = 1, \dots, q,$$

with the s_1, \dots, s_q pairwise distinct and $C_{bl}(s_l) \neq 0$ given, then $\zeta = 1$ and

$$f = \tilde{f}.$$

Proof. This is an immediate consequence of Lemma 10 and Proposition 11: Indeed, Lemma 10 ensures that the assumptions of Proposition 11 are satisfied provided that 1.) and 2.) hold. In case $\tilde{p} \leq p$ the result immediately follows from Propositions 11 and 13. In case $\tilde{p} > p$ it follows from interchanging the roles of the two configurations and again applying Propositions 11 and 13. \square

Remark 15 (Interpretation for practical application). *Besides putting some basis assumptions on the ground truth-configuration and requiring positivity of the metabolic parameters, the previous theorem can be read as follows: If one obtains a configuration that matches the measured data, it can be guaranteed to coincide with ground-truth configuration if at least $\tilde{p}+3$ of the found terms $\tilde{k}_2^i + \tilde{k}_3^i$ and \tilde{k}_3^i are pairwise distinct.*

Remark 16 (Generalization for nontrivial fractional blood volume). *Following standard approaches in quantitative PET modeling, we assume here that the PET images provide exactly the tissue concentration C_{tis} . A more realistic model would be that the voxel measurements provide a convex combination of the tissue and blood tracer concentration given by $C_{PET}(t) = (1 - fbv) \cdot C_{tis}(t) + fbv \cdot C_{bl}(t)$, where fbv with $0 \leq fbv \leq 0.05$ describes the fractional blood volume. In case the parameter fbv is known and C_{bl} is available at the same time points as the PET image measurements, our results cover also this setting. The general case, where both fbv and C_{bl} are unavailable, can be addressed by similar techniques as in the proof of Proposition 11. Here, the idea would be to employ a polyexponential parametrization also for C_{bl} , and assuming enough measurements of C_{PET} to be available in order to apply the unique interpolation result of Lemma 8. One would further have to ensure positivity of C_{bl} , the initial condition $C_{bl}(0) = 0$ and conditions on the attenuation $f = C_{art}/C_{bl}$ such as monotonicity and limiting conditions with respect to time approaching zero and infinity, respectively. These requirements imply corresponding conditions on the parameters of C_{art} and C_{bl} .*

4 A Tikhonov approach for parameter identification with noisy data

In the previous section we have established that, under appropriate conditions, the parameters (K_1^i, k_2^i, k_3^i) of the irreversible two tissue compartment model in regions $i = 1, \dots, n$ can be obtained uniquely from measurements $C_{tis}(t_i)$, $i = 1, \dots, T$ and measurements $C_{bl}(s_i)$ for $i = 1, \dots, q$. While this result shows that parameter identification is possible in principle, it considers the idealized scenario of exact measurements. In this section, we consider the situation of noisy measurements, for which we develop a Tikhonov approach for stable parameter identification. As main analytic results of this section, we show i) a stability result, i.e., that the proposed Tikhonov approach is stable with respect to (noise) variations in the measurements (see Theorem 18) and ii) a consistency result, i.e., that in the limit of vanishing noise, solutions of the Tikhonov approach converge to the ground truth parameters (see Theorem 20).

As first step, we define a forward model that maps the unknown parameters to the available measurement data. To this aim, we define the arterial concentration as mapping

$$C_{\text{art}} : \mathbb{R}^p \times \mathbb{R}^p \rightarrow \mathcal{P}_p$$

$$(\lambda, \mu) \mapsto \left[t \mapsto \sum_{i=1}^p \lambda_i e^{\mu_i t} \right].$$

Further, we define a parametrized parent plasma fraction as mapping

$$f : \mathcal{M} \subset \mathbb{R}^{\hat{q}} \rightarrow F_q$$

$$m \mapsto f_m. \quad (17)$$

where $\mathcal{M} \subset \mathbb{R}^{\hat{q}}$ is some (finite dimensional) parameter space and F_q is a degree- q parametrized set of functions.

Remark 17 (Parent plasma fraction example). *A classical model for the parent plasma fraction (see [16] for different models), that we will also use in our numerical experiments below, is the biexponential model*

$$f(t) = Ae^{\xi_1 t} + (1 - A)e^{\xi_2 t} \quad \text{for } t \geq 0.$$

Here $\mathcal{M} = [0, \infty) \times (-\infty, 0]^2$ and the degree of F_q is $q = 4$.

In addition to the parameters of the functions modeling the arterial concentration and the parent plasma fraction, the forward model also includes the parameters $\mathbf{K}^i = (K_1^i, k_2^i, k_3^i)$ for $i = 1, \dots, n$ compartments. With this, the unknown parameters are summarized by $(\lambda, \mu, m, \mathbf{K}^1, \dots, \mathbf{K}^n)$ and we denote by $X = \mathbb{R}^p \times \mathbb{R}^p \times \mathbb{R}^{\hat{q}} \times \mathbb{R}^{3 \times n}$ the resulting parameter space with norm

$$\|(\lambda, \mu, m, \mathbf{K}^1, \dots, \mathbf{K}^n)\|_X^2 := \sum_{j=1}^p (|\lambda_j|^2 + |\mu_j|^2) + \|m\|_2^2 + \sum_{i=1}^n \|\mathbf{K}^i\|_2^2,$$

where $\|\cdot\|_2$ denotes the Euclidean norm. Given measurement points t_1, \dots, t_T for C_{tis} and s_1, \dots, s_q for the total concentration C_{bl} , those parameters are mapped forward to a measurement space $Y = \mathbb{R}^{n \times T + q}$, again equipped with the Euclidean norm $\|\cdot\|_Y = \|\cdot\|_2$ via the function

$$F : \mathcal{D}(F) := \mathbb{R}^p \times \mathbb{R}^p \times \mathcal{M} \times [\epsilon, \infty)^{3 \times n} \subseteq X \rightarrow Y$$

$$x \mapsto (F^1(x), F^2(x)) \quad (18)$$

where, for $x = (\lambda, \mu, m, \mathbf{K}^1, \dots, \mathbf{K}^n)$

$$F^1(x) = \begin{pmatrix} C_{\text{tis}}(C_{\text{art}}(\lambda, \mu), \mathbf{K}^1, \cdot)(t_1) & \dots & C_{\text{tis}}(C_{\text{art}}(\lambda, \mu), \mathbf{K}^1, \cdot)(t_T) \\ \vdots & \ddots & \vdots \\ C_{\text{tis}}(C_{\text{art}}(\lambda, \mu), \mathbf{K}^n, \cdot)(t_1) & \dots & C_{\text{tis}}(C_{\text{art}}(\lambda, \mu), \mathbf{K}^n, \cdot)(t_T) \end{pmatrix} \quad (19)$$

and

$$F^2(x) = (C_{\text{bl}}(s_1) f_m(s_1) - C_{\text{art}}(\lambda, \mu)(s_1) \quad \dots \quad C_{\text{bl}}(s_q) f_m(s_q) - C_{\text{art}}(\lambda, \mu)(s_q)). \quad (20)$$

Here $C_{\text{tis}}(C_{\text{art}}(\lambda, \mu), \mathbf{K}^i, \cdot)$ denotes the solution of the irreversible two tissue compartment ODE model (S) with parameters \mathbf{K}^i and arterial concentration $C_{\text{art}}(\lambda, \mu)$. Note that F^2 depends on the data C_{bl} that must be obtained from blood samples or PET measurements, which we assume

to be given throughout this section. A further adaption of the model to include also C_{bl} as possibly noise measurement is possible with the same techniques as below, but will be omitted for the sake of simplicity.

Now denoting by $\hat{C}_{\text{tis}}^i(t_1), \dots, \hat{C}_{\text{tis}}^i(t_T)$ for $i = 1, \dots, n$ measurements corresponding to the ground-truth parameters, our goal is to find parameters $(\lambda, \mu, m, \mathbf{K}^1, \dots, \mathbf{K}^n)$ such that

$$F(\lambda, \mu, m, \mathbf{K}^1, \dots, \mathbf{K}^n) = \begin{pmatrix} \hat{C}_{\text{tis}}^1(t_1) & \dots & \hat{C}_{\text{tis}}^1(t_T) \\ \vdots & \ddots & \vdots \\ \hat{C}_{\text{tis}}^n(t_1) & \dots & \hat{C}_{\text{tis}}^n(t_T) \end{pmatrix} \times (0, \dots, 0) \in \mathbb{R}^{n \times T} \times \mathbb{R}^q.$$

Accounting for the fact that the given parameters are perturbed by measurement noise, i.e., we are actually given $(C_{\text{tis}}^i)^\delta(t_l)$ with

$$\sum_{i=1}^n \sum_{l=1}^T \|(C_{\text{tis}}^i)^\delta(t_l) - \hat{C}_{\text{tis}}^i(t_l)\|_2^2 \leq \delta,$$

we address the parameter identification problem via a minimization problem of the form

$$\min_{(\lambda, \mu, m, \mathbf{K}^1, \dots, \mathbf{K}^n) \in \mathcal{D}(F)} \|F(\lambda, \mu, m, \mathbf{K}^1, \dots, \mathbf{K}^n) - (C_{\text{tis}}^\delta, 0)\|_Y^2 + \alpha \|(\lambda, \mu, m, \mathbf{K}^1, \dots, \mathbf{K}^n) - (\bar{\lambda}, \bar{\mu}, \bar{m}, \bar{\mathbf{K}}^1, \dots, \bar{\mathbf{K}}^n)\|_X^2. \quad (21)$$

Here $0 \in \mathbb{R}^q$ is a q -dimensional vector of zeros, C_{tis}^δ summarizes the available measurements for C_{tis}^δ , i.e.,

$$C_{\text{tis}}^\delta = \begin{pmatrix} (C_{\text{tis}}^1)^\delta(t_1) & \dots & (C_{\text{tis}}^1)^\delta(t_T) \\ \vdots & \ddots & \vdots \\ (C_{\text{tis}}^n)^\delta(t_1) & \dots & (C_{\text{tis}}^n)^\delta(t_T) \end{pmatrix}.$$

and $(\bar{\lambda}, \bar{\mu}, \bar{m}, \bar{\mathbf{K}}^1, \dots, \bar{\mathbf{K}}^n)$ is an initial guess on the ground truth parameters. The above approach corresponds to *Nonlinear Tikhonov-Regularisation*, for which stability and consistency results can be ensured as follows.

Theorem 18 (Well-posedness and stability). *Let the parent plasma fractions f_m be such that the mapping $m \mapsto f_m(t)$ is continuous for any $t \in [0, \infty)$. Then, for any given datum C_{tis}^δ , the minimization problem (21) admits a solution. Moreover, solutions are stable in the sense that, if $(C_{\text{tis}}^{\delta_k})_k$ is a sequence of data converging to some datum C_{tis}^δ , then, any sequence of solutions $(x^k)_k$ of (21) with data $(C_{\text{tis}}^{\delta_k})_k$ admits a convergent subsequence, and the limit of any convergent subsequence x is a solution of (21) with data C_{tis}^δ .*

Proof. Since X and Y are finite dimensional and $D(F)$ is obviously closed, this follows from classical results in regularization theory, see for instance [4, Theorem 10.2] provided that F is continuous.

We start with continuity of F^1 as in (19), the first component of F . For this, it suffices to show that the mapping from the parameter $(\lambda, \mu, \mathbf{K}^1, \dots, \mathbf{K}^n)$ to $C_{\text{tis}}^i(t)$, with $t \in [0, \infty)$ fixed, is continuous, which, in turn, follows from the representation of $C_{\text{tis}}^i(t)$ as in (1) if, for any $g \in L^2(0, t)$ and any sequence $(\lambda^l, \mu^l)_l$ converging to (λ, μ) it holds that

$$\int_0^t g(s) (C_{\text{art}}(\lambda^l, \mu^l) - C_{\text{art}}(\lambda, \mu))(s) ds \rightarrow 0 \quad \text{as } l \rightarrow \infty. \quad (22)$$

By Hölder's inequality, the latter follows from $C_{\text{art}}(\lambda^l, \mu^l) \rightarrow C_{\text{art}}(\lambda, \mu)$ in $L^2(0, T_{\max})$, which, in turn, follows via the Lebesgue dominated convergence theorem from point-wise convergence of $C_{\text{art}}(\lambda^l, \mu^l)$ and the fact that $|C_{\text{art}}(\lambda^l, \mu^l)|$ on $[0, t]$ can easily be bounded by a constant independent of l .

Regarding F^2 as in (20), the second component of F , continuity immediately follows from continuity of $(\lambda, \mu) \mapsto C_{\text{art}}(\lambda, \mu)(t)$ and $m \mapsto f_m(t)$ for any $t \in [0, \infty)$ fixed, where the latter holds by assumption. \square

Remark 19 (Continuity of $m \mapsto f_m(t)$). *Note that the assumption of continuity of $m \mapsto f_m(t)$ is only necessary since we allow for arbitrarily parametrized parent plasma fractions; it holds in particular for the biexponential model of Remark 17 and will typically hold for any reasonable parametrization.*

At last in this section we now establish a consistency result.

Theorem 20 (Consistency). *Let $(\hat{p}, n, ((\hat{\lambda}_j, \hat{\mu}_j))_{j=1}^{\hat{p}}, ((\hat{K}_1^i, \hat{k}_2^i, \hat{k}_3^i))_{i=1}^n, (\hat{C}_{tis}^i)_{i=1}^n, \hat{C}_{art})$ be a ground-truth configuration of the irreversible two tissue compartment model satisfying the assumptions of Theorem 14, and let $f_{\hat{m}} \in \mathcal{M}$ be a ground-truth parent plasma fraction.*

With $\hat{x} = (\hat{\lambda}, \hat{\mu}, \hat{m}, \hat{\mathbf{K}}^1, \dots, \hat{\mathbf{K}}^n)$ the corresponding parameters and $\hat{y} := F(\hat{x})$ the corresponding measurement data, let y^{δ_k} be any sequence of noisy data such that $\|\hat{y} - y^{\delta_k}\| \leq \delta_k$ with $\delta_k > 0$, $\lim_{k \rightarrow \infty} \delta_k = 0$.

Then, any sequence of solutions $(x_k)_k$ of (21) with data $y^\delta = y^{\delta_k}$ and $\alpha = \alpha_k$ such that $\alpha_k \rightarrow 0$ and $\delta_k^2/\alpha_k \rightarrow 0$ as $k \rightarrow \infty$ admits a convergent subsequence. Any limit $x = (\lambda, \mu, m, \mathbf{K}^1, \dots, \mathbf{K}^n)$ of such a subsequence, such that the corresponding parameter configuration satisfies the assumptions of Theorem 14, coincides with \hat{x} . Further, if any limit of a convergent subsequence corresponds to a parameter configuration satisfying the assumptions of Theorem 14, then the entire sequence $(x_k)_k$ converges to \hat{x} .

Proof. This is a consequence of Theorem 14, which ensures that there is a unique $x \in X$ with $F(x) = \hat{y}$, and of classical results from regularization theory, see for instance [4, Theorem 10.3]. \square

Remark 21 (Interpretation of the consistency result). *When choosing $p \geq 3$ and $n \geq 3$, and given the definition of $\mathcal{D}(F)$ as in (18), the above consistency result together with the unique reconstructability result of Theorem 14 can be interpreted as follows: Whenever the parameters $(K_1^i, k_2^i, k_3^i)_{i=1}^n$ corresponding to a limit x of $(x_k)_k$ are such that at least $p + 3$ of the parameters k_3^i and $k_2^i + k_3^i$ are pairwise distinct, then one can ensure that $x = \hat{x}$.*

Remark 22 (Multi-parameter regularization). *The setting of (21) and the subsequent results on well-posedness and consistency can be generalized to incorporating different regularization parameters for the different norms and data terms, see for instance [6], which is reasonable given the fact that the parameters might live on different scales, and given the fact that the noise level of different measurements over time might be different.*

Remark 23 (Model Variations). *Currently, in the setting of (21), the parameters $(K_1^i, k_2^i, k_3^i)_{i=1}^n$ are bounded away from zero by $\epsilon > 0$. For the $(\mu_j)_{j=1}^p$, we currently do not pose any constraints even though, as mentioned in Remark 6, only the choice $\mu_j < 0$ is reasonable from a physiological perspective. Likewise, C_{art} as parametrized in (17), does not necessarily satisfy $C_{\text{art}}(0) = 0$. These two conditions, however, can be easily incorporated in the model via the additional constraint $\mu_j \leq -\tilde{\epsilon}$ for some $\tilde{\epsilon} \geq 0$ and via setting $\lambda_p = -\sum_{j=1}^{p-1} \lambda_j$, respectively.*

5 Numerical solution algorithm

In this section, we provide proof-of-concept numerical experiments that illustrate the analytic unique identifiability results of Sections 3 and 4 also numerically.

5.1 Experimental setup

We consider the following experimental setup: As ground truth data, we consider $n = 3$ different anatomical regions, where, based on the realistic values provided in [8, Table 1], the parameters are chosen as

$$\begin{pmatrix} K_1^1 \\ k_2^1 \\ k_3^1 \end{pmatrix} = \begin{pmatrix} 0.157 \\ 0.174 \\ 0.118 \end{pmatrix}, \quad \begin{pmatrix} K_1^2 \\ k_2^2 \\ k_3^2 \end{pmatrix} = \begin{pmatrix} 0.161 \\ 0.179 \\ 0.096 \end{pmatrix} \quad \text{and} \quad \begin{pmatrix} K_1^3 \\ k_2^3 \\ k_3^3 \end{pmatrix} = \begin{pmatrix} 0.177 \\ 0.159 \\ 0.088 \end{pmatrix}. \quad (23)$$

Here, region 1 corresponds to the frontal cortex, region 2 to the temporal cortex and region 3 to the occipital cortex in the human brain. We model the true arterial concentration by the triexponential function given by

$$C_{\text{art}}(t) = -5e^{-0.5t} + 4e^{-0.2t} + e^{-0.1t}$$

and the parent plasma fraction for the biexponential model by

$$f(t) = 0.1e^{-0.005t} + 0.9e^{-0.1t}$$

for $0 \leq t \leq T_{\text{max}}$ where $T_{\text{max}} = 3750 \text{ sec} \hat{=} 62.5 \text{ min}$. See Figure 2 for the visualisation of the parent plasma fraction, the arterial concentration and the measured total and additive concentrations. We assume that we conduct a PET examination for $T = 25$ time frames where, equidistantly distributed, six take place in the first minutes, four in the following two minutes, two in the next two minutes, three in the next 7.5 minutes and finally ten in the remaining 50 minutes. Regarding C_{bl} , we assume that measurements $C_{\text{bl}}(s_1), \dots, C_{\text{bl}}(s_q)$ are available at the same timepoints $0 = t_1, \dots, t_T$ at which measurements of C_{tis} are available, i.e., $q = T$. This reflects the situation that an estimate of the total arterial tracer concentration is obtained from the PET images (rather than blood sampling), a technique that for which many recent works exist [18]. In view of Propositions 11 and 13, the above experimental setting satisfies the assumptions such that unique identifiability from noiseless data can be guaranteed.

We summarize the unknown parameters of this setting by

$$x^\dagger = (\lambda_1, \lambda_2, \lambda_3, \mu_1, \mu_2, \mu_3, m_1, m_2, m_3, K_1^1, k_2^1, k_3^1, K_1^2, k_2^2, k_3^2, K_1^3, k_2^3, k_3^3)^T \in \mathbb{R}^{18},$$

where x^\dagger denotes the ground-truth parameters as specified above. For a given number of measurements $T \in \mathbb{N}$, the data is summarized in vectorized form via

$$y^\dagger = (y_1, 0) = F(x^\dagger) \in \mathbb{R}^{3T+T},$$

where, abusing notation, $F : \mathbb{R}^{18} \rightarrow \mathbb{R}^{3T+T}$ is a vectorized version of the forward model of (18).

For the subsequent numerical experiments, we will also consider noisy versions of the data, denoted by y^{δ_y} with δ_y being the noise level. Those are defined by adding Gaussian noise with zero mean and variance $\frac{\delta_y^2}{3T}$ to each of the first $3T$ entries of y^\dagger (note that no noise is added to the zero-entries), i.e., $(y^\delta)_l = y_l^\dagger + \eta_l$ with $\eta_l \sim \mathcal{N}\left(0, \frac{\delta_y^2}{3T}\right)$ for $l = 1, \dots, 3T$, such that

$$\mathbb{E}(\|y^\delta - y^\dagger\|_Y^2) = \sum_{l=1}^{3T} \mathbb{E}(\eta_l^2) = \sum_{l=1}^{3T} \frac{\delta_y^2}{3T} = \delta_y^2.$$

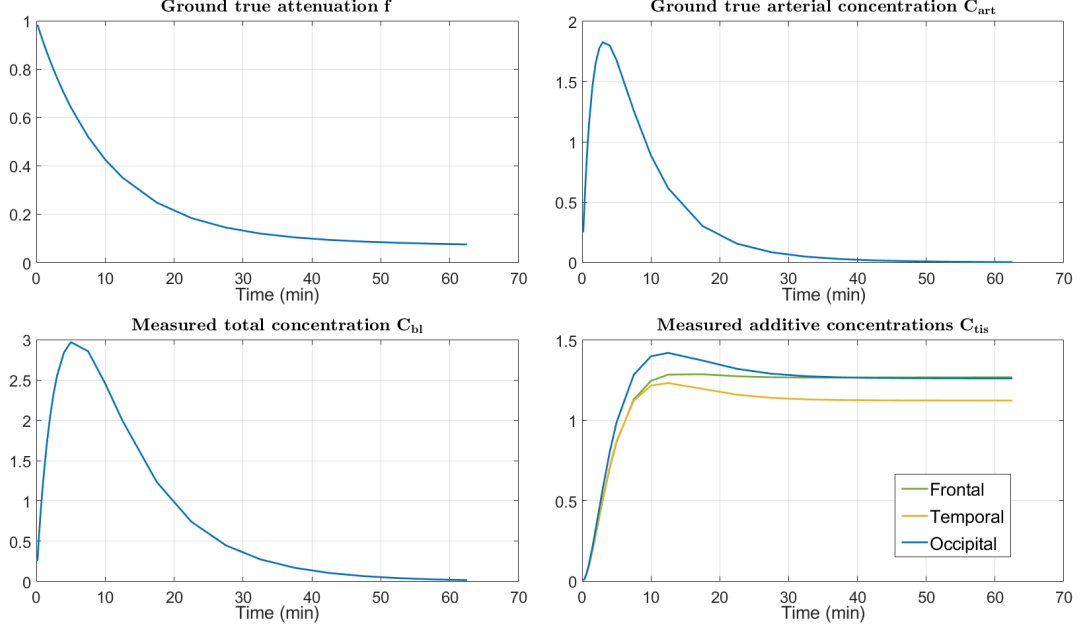


Figure 2: The evolutions in the first two plots display the ground true parent plasma fraction and arterial concentration. The third and fourth plot correspond to the resulting simulated measurements of the total and additive concentrations depending on the parent plasma fraction and the arterial concentration.

where $\mathbb{E}(\cdot)$ denotes the expectation.

As we are dealing with locally convergent methods, it will also be important to choose a reasonable initial guess x_0 for the algorithm. In order to test the performance of the algorithm in dependence on how close the initial guess is to the true solution, we employ the following steps to obtain perturbed initial guesses. Given a level of perturbation δ_x , we define

$$x_0 = x^\dagger(1 + \sigma\gamma) \quad (24)$$

where $\sigma \sim \text{Unif}(\{-1, 1\})$, i.e., is uniformly distributed on $\{-1, 1\}$ and $\gamma \sim \mathcal{N}(\delta_x, \frac{1}{4}\delta_x)$, i.e., is Gaussian distributed with mean δ_x and variance $\delta_x/4$. This results in a expected squared deviation of x_0 from x^\dagger as by

$$\mathbb{E}\left(\frac{\|x_0 - x^\dagger\|_X^2}{\|x^\dagger\|_X^2}\right) = \frac{1}{\|x^\dagger\|_X^2} \sum_{i=1}^{18} (x_i^\dagger)^2 \mathbb{E}(\sigma_i^2 \gamma_i^2) = \mathbb{E}(\gamma_1^2) = \frac{1}{4}\delta_x + \delta_x^2, \quad (25)$$

where $\sigma_i \sim \text{Unif}(\{-1, 1\})$ and $\gamma_i \sim \mathcal{N}(\delta_x, \frac{1}{4}\delta_x)$ for $i = 1, \dots, 18$ are independent random variables.

5.2 Algorithmic implementation

In order to numerically solve the non-linear parameter identification, we employ the *iteratively regularized Gauss-Newton method* of [1], see also [4, Section 11.2]. This is a standard method for

solving non-linear inverse problems. It is related to the Tikhonov approach discussed in Section 4 in the sense that similar results on stability and convergence/consistency (under appropriate source conditions) can be obtained, see for instance [2, 5], but different to the Tikhonov approach, regularization is achieved by early stopping of the algorithm rather than adding an additional penalty term to the data-fidelity term. Early stopping has the advantage that, using an estimate of the noise level of the data, the discrepancy principle [4, Section 4.3] can be used to determine the appropriate amount of regularization, without requiring multiple solutions of a minimization problem as would be the case with the Tikhonov approach.

Given an initial guess $x_0 \in \mathcal{D}(F)$ and a sequence of regularization parameters $(\alpha_k)_k$ such that

$$\alpha_k > 0, \quad 1 \leq \frac{\alpha_k}{\alpha_{k+1}} \leq c_\alpha, \quad \lim_{k \rightarrow \infty} \alpha_k = 0, \quad (26)$$

where $c_\alpha > 1$ is some constant, the iteration steps of the iteratively regularized Gauss-Newton method for $k = 0, 1, 2, \dots$ are given as

$$x_{k+1}^\delta = x_k^\delta + \left(F' [x_k^\delta]^T F' [x_k^\delta] + \alpha_k I \right)^{-1} \left(F' [x_k^\delta]^T (y^\delta - F(x_k^\delta)) + \alpha_k (x_0 - x_k^\delta) \right), \quad (27)$$

where $F' [x_k^\delta] \in \mathbb{R}^{(nT+q) \times (2p+3+2n)}$ denotes the Jacobian Matrix of F at x_k^δ and $F' [x_k^\delta]^T$ its transpose.

Those iteration steps are repeated until the *discrepancy principle* is satisfied, that is, until $\|F(x_k^\delta) - y^\delta\|_Y \leq \tau \delta$ holds for the first time, where δ is an estimate of $\|y^\delta - y^\dagger\|_Y$ and $\tau > 1$ with $\tau \approx 1$ is a parameter. The iterate x_k is then returned as the approximate solution of $F(x) \approx y^\delta$.

Remark 24 (Guaranteed convergence). *Since the parameter identification problem addressed here is highly non-linear, global convergence guarantees for any numerical solution algorithm are out of reach. For the iteratively regularized Gauss-Newton method together with the discrepancy principle, as considered here, at least local convergence guarantees can be obtained as long as a particular source condition, i.e., a regularity condition on the ground truth solution holds, see [5] for details.*

In a practical application, the iteration (27) is combined with a projection on $\mathcal{D}(F)$, which is a closed, convex set for which the projection is explicit (we denote the projection map by $\mathcal{P}_{\mathcal{D}(F)}$), see [9, Theorem 4] for corresponding results on convergence of such a projected method. Together with this, we arrive at the algorithm for solving $F(x) \approx y^\delta$ as provided in Algorithm 1, where we set $\epsilon = 10^{-3}$ for defining $\mathcal{D}(F) = \mathbb{R}^3 \times \mathbb{R}^3 \times [0, \infty) \times (-\infty, 0]^2 \times [\epsilon, \infty)^{3T}$.

For the regularization parameters $(\alpha_i)_i$ we choose the ansatz

$$\alpha_i = a e^{-bi} \quad (28)$$

for $i \in \mathbb{N}$ where $a = 800$ and $b = 1/5$ are fixed parameters. Besides fulfilling the decay conditions of (26), this choice is motivated by the goal of penalizing deviations from the initial guess rather strongly at early iterations (a large), and avoiding an exploding condition number of the matrix $\left(F' [x_k^\delta]^T F' [x_k^\delta] + \alpha_k I \right)$, that needs to be inverted at each iteration, during later iterations (b rather small).

For the realization of the forward operator F and the adjoint of its Fréchet-Differential the main idea is to vectorise the computations and omit expensive for-loops. For that, one may exploit that the entries of $F(x)$ and $F'[x]^*$, which mostly consist of integral type entities, may be computed analytically. The elementary components are of the form $\int e^{\mu s} ds$, $\int e^{(k_2+k_3)(s-t)} e^{\mu s} ds$, $\int s e^{(k_2+k_3)(s-t)} e^{\mu s} ds$ and $\int s e^{\mu s} ds$. The latter may be computed by hand applying integration by parts. The corresponding terms, which depend on a combination of

Algorithm 1 Parameter Identification by IRGNM

Input: $\delta_x, \delta_y > 0, \tau > 1, (\alpha_i)_i,$
 $x_0 \in \mathcal{D}(F), y^\delta \in Y, (C_{bl}(t_j))_{j=1}^T$
Initialise: $r_0 \leftarrow y^\delta - F(x_0)$
 $i \leftarrow 0$
while $\|r_i\|_Y > \tau\delta_y$ **do**
 $\mathcal{A} \leftarrow F'[x_i]^*$
 $\mathcal{B} \leftarrow \mathcal{A}\mathcal{A}^*$
Solve $\mathcal{B}(x - x_i) = \mathcal{A}r_i + \alpha_i(x_0 - x_i)$ *for* $x \in X$
 $x_{i+1} \leftarrow \mathcal{P}_{\mathcal{D}(F)}(x)$
 $r_{i+1} \leftarrow y^\delta - F(x_{i+1})$
 $i \leftarrow i + 1$
end while
return x_k

time evaluations, region and polyexponential parameters of C_{art} , are saved in three-dimensional tensors which are overloaded throughout a respective iteration to finally build up the adjoint operator of the Fréchet-Differential. For the implementation of the IRGNM we will use the computational software MATLAB (see [11]).

6 Experimental results

In order to evaluate the identifiability of the parameters x^\dagger from noisy data $y^\delta \approx F(x^\dagger)$, we consider both the situation of noiseless data ($\delta_y = 0$) and different noise levels $\delta_y \in \{10^{-4}, 10^{-3}, 10^{-2}\}$. For the latter, it is important to note that, relative to the magnitude of the data, the noise level $\delta_y = 10^{-2}$ is already rather high. Indeed, as can be observed in Figure 3, which depicts the average magnitudes of different regions in the data, about 25% of the measurements have a magnitude below 10^{-1} . For those values, adding Gaussian noise with standard deviation $\delta_y = 10^{-2}$, for instance, results in noisy data whose standard deviation is already between 10% and 100% of the magnitude of the data itself.

For defining the initialization of the algorithm, we test with perturbations of the ground truth as defined in (24) for $\delta_x \in \{0.01, 0.05, 0.1, 0.15\}$. Recall that those are relative perturbations such that the square root of the expected squared deviation from the ground truth x^\dagger is between $\approx 5\%$ for $\delta_x = 0.01$ and $\approx 25\%$ for $\delta_x = 0.15$.

To quantify the improvement compared to the initialization that is obtained by the algorithm, in addition to plotting the residual value $\|F(x_k) - y^\delta\|_Y$ and the relative error $\frac{\|x_k - x^\dagger\|_X}{\|x^\dagger\|_X}$ over iterations, we provide the following two values:

$$\rho_{opt} = 100 \left(1 - \|x_0^\delta - x^\dagger\|_X^{-1} \min_{1 \leq k \leq iter_{max}} \|x_k^\delta - x^\dagger\|_X \right)$$

provides the best possible improvement (in percent, relative to the initialization) that was obtained during all iterations, and

$$\rho_d = 100 \left(1 - \|x_0^\delta - x^\dagger\|_X^{-1} \|x_N^\delta - x^\dagger\|_X \right) \%$$

provides the improvement that was obtained at iteration N where the algorithm was stopped by the discrepancy principle, i.e., the first iteration N where $\|F(x_N^\delta) - y^\delta\|_Y \leq \tau\delta$ was fulfilled.

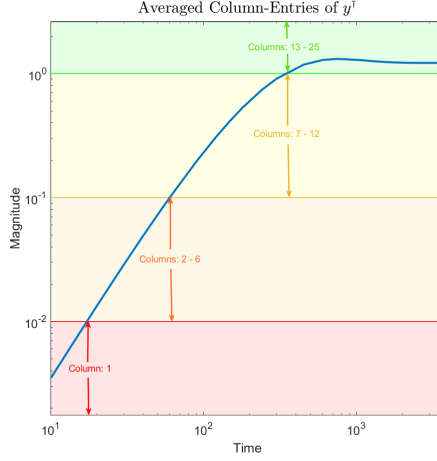


Figure 3: Visualization of magnitudes occurring in different time-intervals (i.e., columns) of the data y^\dagger

Table 1: Number (full setting/setting with known C_{art}) of experiments (out of ten) not included in the final evaluation due to divergence.

	$\delta_x = 0.15$	$\delta_x = 0.1$	$\delta_x = 0.05$	$\delta_x = 0.01$
$\delta_y = 0$	0/0	0/0	0/0	0/0
$\delta_y = 10^{-4}$	77/36	65/17	30/2	4/0
$\delta_y = 10^{-3}$	58/21	40/8	18/1	2/0
$\delta_y = 10^{-2}$	32/14	29/4	13/1	2/0

Experiments were carried out for each combination of δ_y and δ_x as above. In order to obtain representative results, each experiment was carried out 100 times. Those experiments where the algorithm diverged (i.e., no improvement compared to the initialization was achieved) were dropped (see Table 1 for the number of dropped experiments for each parameter combination) and, among the remaining ones, the one whose performance was closest to the median performance of all repetitions was selected for the figures below.

Figures 4 to 7 show the result obtained for different choices of $\delta_y = 0, 10^{-4}, 10^{-3}, 10^{-2}$. In those figures, the top and bottom rows depict the evaluation of the residual value $\|F(x_k) - y^\delta\|_Y$ and the relative error $\frac{\|x_k - x^\dagger\|_X}{\|x^\dagger\|_X}$ over iterations, respectively, both with a logarithmic scale for the vertical axis. The different columns show results for the different choices of $\delta_x = 0.15, 0.1, 0.05, 0.01$. The values of ρ_{opt} and ρ_d (the latter only for $\delta_y > 0$), together with the respective iterations, are provided at the top of plots of the second row. Note that, while the algorithm was always run until a fixed, maximal number of iterations (300 for $\delta_y = 0$ and 200 for $\delta_y > 0$) for obtaining the figures, in practice the iterations would be stopped by the discrepancy principle for $\delta_y > 0$. For $\delta_y > 0$, the red lines always indicate the levels of the residual value (top row) and iteration number (bottom row) where the algorithm would have stopped according to the discrepancy principle.

In Figure 4, which considers the noiseless case, one can observe that the ground truth pa-

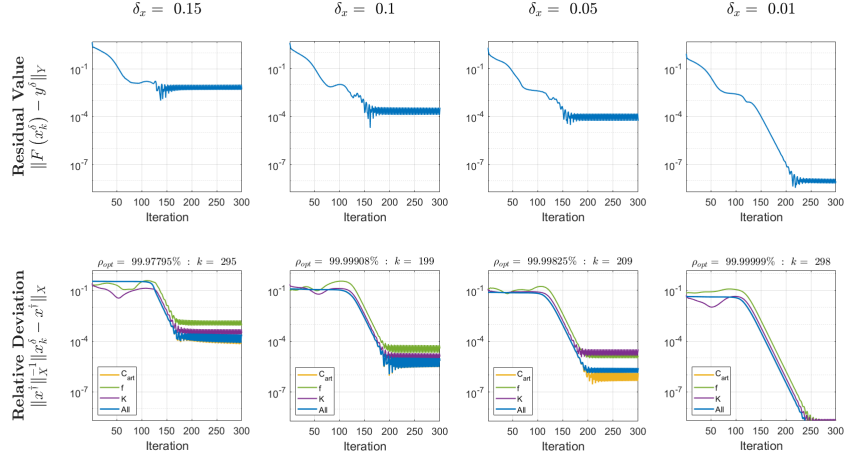


Figure 4: Performance of IRGNM for $\delta_y = 0$ and different initial guesses

rameters x^\dagger are approximated very well for all levels of δ_x . This confirms our analytic unique identifiability result also in practice.

Considering Figures 5 to 7, one can observe that, in the low noise regime, a good approximation of the ground truth x^\dagger is still possible across different values of δ_x . For higher noise, a good initialization (i.e., a small value of δ_x) is of increasing importance and, in some cases, in particular for $\delta_y = 10^{-2}$ and the parameters of the parent plasma fraction f , the ground truth can not be recovered reasonably well.

In a second set of experiments, we consider the situation that not only C_{bl} , but also measurements of the values of C_{art} are available at the time-points t_1, \dots, t_T . While it is possible in practice to obtain those values via blood sample analysis, this procedure is time consuming and expensive, such that it is a relevant question to what extent such samples improve the identifiability of the tissue parameters.

Again, for each combination of δ_y and δ_x , each experiment was carried out 100 times, the number of divergent experiments is shown in Table 1 and the Figures show the experiment whose performance was closest to the median performance of the non-divergent experiments.

Results are shown in Figures 8 to 11, where the quantities shown in and above the plots are the same as in Figures 4 to 7. It can be observed that the performance with known C_{art} is improved compared to the situation where only C_{bl} is known, across all choices of δ_y and δ_x . While for $\delta_y \in \{0, 10^{-4}\}$, both versions yield acceptable results, for $\delta_y \in \{10^{-3}, 10^{-2}\}$ knowledge of C_{art} enables a good approximation of the ground truth parameters in situations where this was not possible with knowing only C_{bl} . This indicates that, as one would expect, the problem of also identifying f from measurements is significantly more difficult and there is a benefit (at least for this solution methods) in measuring C_{art} via blood samples.

7 Conclusions

In this work, we have shown that most tissue parameters of the irreversible two-tissue compartment model in quantitative PET imaging can, in principle, be recovered from standard PET measurements only. Furthermore, a full recovery of all parameters is possible provided that suf-

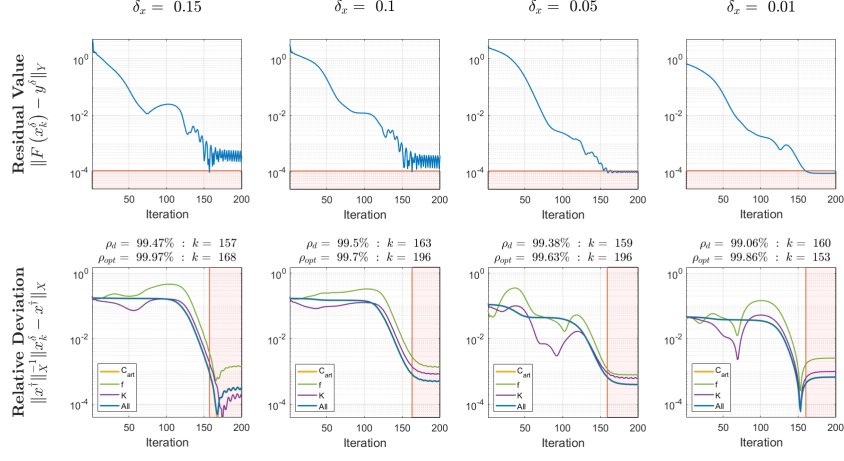


Figure 5: Performance of IRGNM for $\delta_y = 10^{-4}$ and different initial guesses

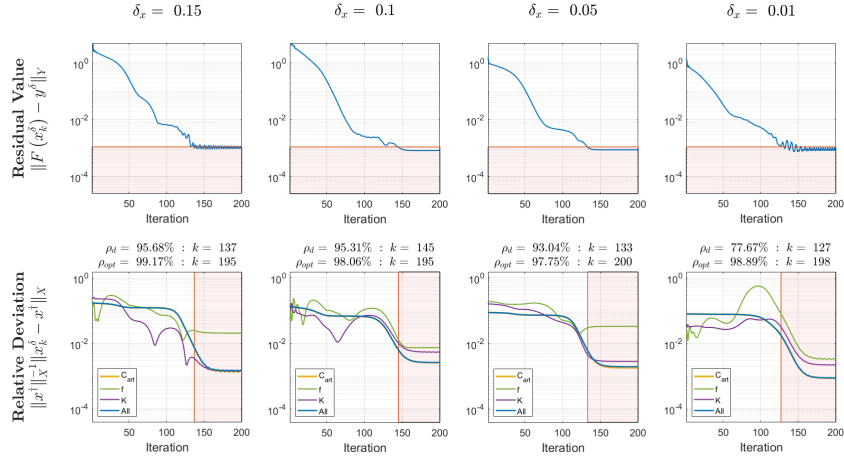


Figure 6: Performance of IRGNM for $\delta_y = 10^{-3}$ and different initial guesses

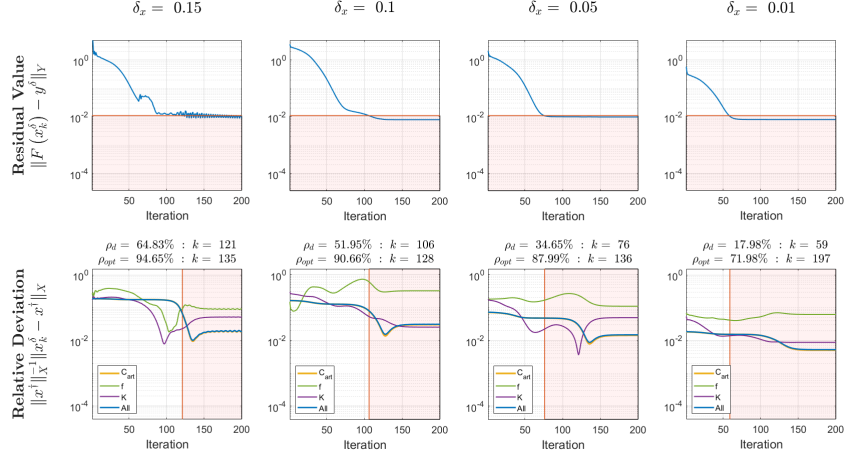


Figure 7: Performance of IRGNM for $\delta_y = 10^{-2}$ and different initial guesses

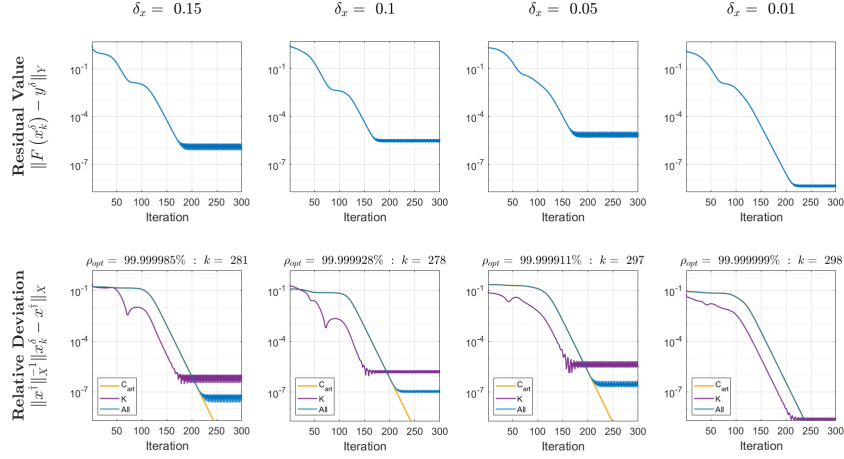


Figure 8: Performance of IRGNM for $\delta_y = 0$ and different initial guesses and known parent plasma fraction f

ficiently many measurements of the total arterial concentration are available. This is important, since it shows that parameter recovery is possible via using only quantities that are easily obtainable in practice, either directly from the acquired PET images or with a relatively simple analysis of blood samples. While these results consider the idealized scenario of noiseless measurements, we have further shown that standard Tikhonov regularization applied to this setting yields a stable solution method that is capable of exact parameter identification in the vanishing noise limit.

These findings open the door to a comprehensive numerical investigation of parameter identification based on only PET measurements and estimates of the total arterial tracer concentration,

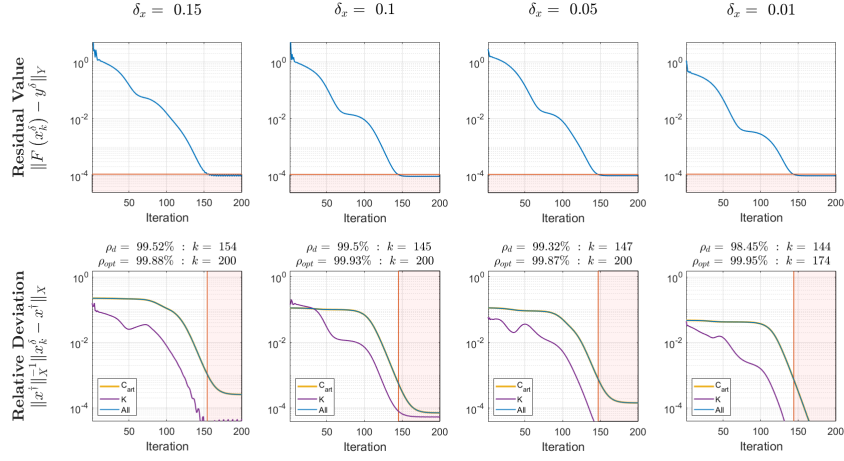


Figure 9: Performance of IRGNM for $\delta_y = 10^{-4}$ and different initial guesses and reduced operator

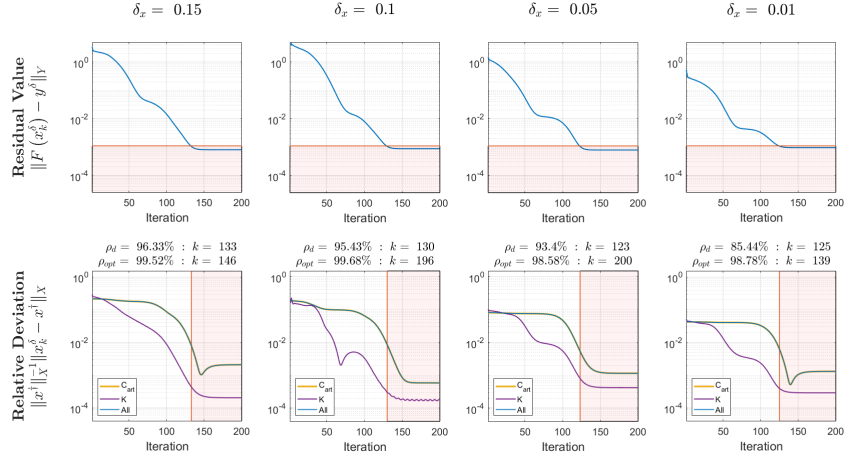


Figure 10: Performance of IRGNM for $\delta_y = 10^{-3}$ and different initial guesses and reduced operator

using real measurement data and advanced numerical algorithms. While the numerical results in this paper provide a first indication that it can be possible to transfer our analytical results to concrete applications, we expect that a comprehensive effort is necessary to obtain a practically usable numerical framework for parameter identification. This will be the next step of our research in that direction.

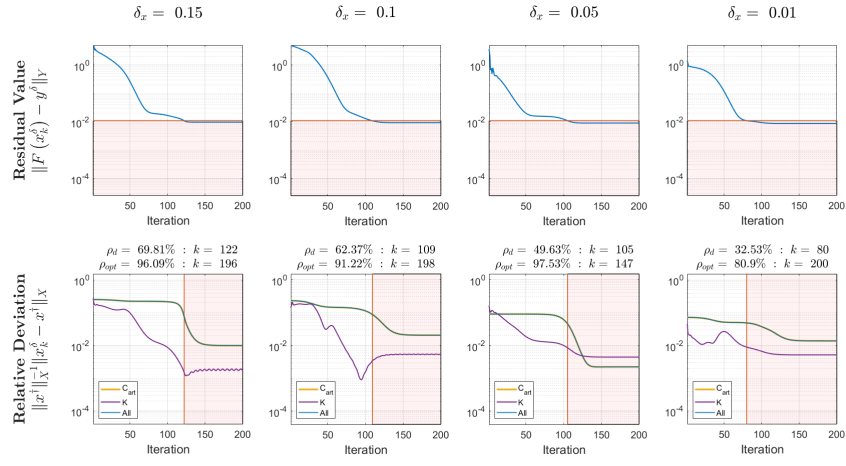


Figure 11: Performance of IRGNM for $\delta_y = 10^{-2}$ and different initial guesses and reduced operator

References

- [1] A. B. BAKUSHINSKII, *The problem of the convergence of the iteratively regularized gauss-newton method*, Computational Mathematics and Mathematical Physics, 32 (1992), p. 1353–1359.
- [2] B. BLASCHKE, A. NEUBAUER, AND O. SCHERZER, *On convergence rates for the iteratively regularized gauss-newton method*, IMA Journal of Numerical Analysis, 17 (1994), pp. 421–436.
- [3] Y. CHEN, J. GOLDSMITH, AND R. T. OGDEN, *Nonlinear Mixed-Effects Models for PET Data*, IEEE Transactions on Biomedical Engineering, 66 (2019), pp. 881–891.
- [4] H. W. ENGL, M. HANKE, AND A. NEUBAUER, *Regularization of Inverse Problems*, Springer Science & Business Media, Berlin Heidelberg, 2000.
- [5] T. HOHAGE, *Logarithmic convergence rates of the iteratively regularized gauss - newton method for an inverse potential and an inverse scattering problem*, Inverse Problems, 13 (1997), pp. 1279–1299.
- [6] M. HOLLER, R. HUBER, AND F. KNOLL, *Coupled regularization with multiple data discrepancies*, Inverse Problems, 34 (2018), p. 084003.
- [7] R. HUESMAN AND P. COXSON, *Consolidation of common parameters from multiple fits in dynamic PET data analysis*, IEEE Transactions on Medical Imaging, 16 (1997).
- [8] W. J. JAGUST, J. P. SEAB, R. H. HUESMAN, P. E. VALK, C. A. MATHIS, B. R. REED, P. G. COXSON, AND T. F. BUDINGER, *Diminished glucose transport in alzheimer’s disease: Dynamic pet studies*, Journal of Cerebral Blood Flow and Metabolism, 11 (1991), pp. 323–330.
- [9] B. KALTENBACHER AND A. NEUBAUER, *Convergence of projected iterative regularization methods for nonlinear problems with smooth solutions*, Inverse Problems, 22 (2006), pp. 1105–1119.
- [10] J. LOGAN, J. S. FOWLER, Y.-S. DING, D. FRANCESCHI, G.-J. WANG, N. D. VOLKOW, C. FELDER, AND D. ALEXOFF, *Strategy for the formation of parametric images under conditions of low injected radioactivity applied to PET studies with the irreversible monoamine oxidase a tracers [11c]clorgyline and deuterium-substituted [11c]clorgyline*, Journal of Cerebral Blood Flow & Metabolism, 22, pp. 1367–1376.
- [11] MATLAB, 9.8.0.1721703 (R2020a) Update 7, The MathWorks Inc., Natick, Massachusetts, 2020.
- [12] G. POLYA AND G. SZEGÖ, *Aufgaben und Lehrsätze aus der Analysis - Zweiter Band: Funktionentheorie · Nullstellen Polynome · Determinanten Zahlentheorie*, Springer-Verlag, Berlin Heidelberg New York, 2013.
- [13] R. R. RAYLMAN, G. D. HUTCHINS, R. S. B. BEANLANDS, AND M. SCHWAIGER, *Modeling of Carbon-11-Acetate Kinetics by Simultaneously Fitting Data from Multiple ROIs Coupled by Common Parameters*, Journal of Nuclear Medicine, 35 (1994), pp. 1286–1291.
- [14] L. SOKOLOFF, *Mapping cerebral functional activity with radioactive deoxyglucose*, Trends in Neurosciences, 1, pp. 75–79. Publisher: Elsevier.

- [15] R. TODD OGDEN, F. ZANDERIGO, AND R. V. PARSEY, *Estimation of in vivo nonspecific binding in positron emission tomography studies without requiring a reference region*, NeuroImage, 108 (2015), pp. 234–242.
- [16] M. TONETTO, G. RIZZO, M. VERONESE, M. FUJITA, S. ZOGHBI, P. ZANOTTI-FREGONARA, AND A. BERTOLDO, *Plasma radiometabolite correction in dynamic pet studies: Insights on the available modeling approaches*, Journal of Cerebral Blood Flow & Metabolism, 36 (2015), pp. 326–339.
- [17] M. VERONESE, R. N. GUNN, S. ZAMUNER, AND A. BERTOLDO, *A non-linear mixed effect modelling approach for metabolite correction of the arterial input function in pet studies*, NeuroImage, 66 (2013), pp. 611–622.
- [18] P. ZANOTTI-FREGONARA, K. CHEN, J.-S. LIOW, M. FUJITA, AND R. B. INNIS, *Image-derived input function for brain PET studies: Many challenges and few opportunities*, Journal of Cerebral Blood Flow & Metabolism, 31, pp. 1986–1998.